

PSF depletion on both *Per1* transcription and clock function.

These results establish a specific function for the PER proteins and a molecular mechanism for circadian clock negative feedback, central aspects of clock function that have long been poorly understood. Our analysis indicates that a PER complex rhythmically associates with DNA-bound CLOCK-BMAL1 at the *Per1* promoter and, by virtue of its constituent PSF, recruits the SIN3-HDAC complex and thereby deacetylates histones 3 and 4 and represses transcription (fig. S7). CLOCK preferentially acetylates H3K9 (24), so PER- and PSF-dependent recruitment of the SIN3-HDAC complex could serve to reverse modifications produced by CLOCK, which generates a circadian rhythm of H3K9 acetylation. Our ongoing work indicates that a PER complex has an additional role in negative feedback, acting to repress *Per* and *Cry* transcriptional elongation (15).

The function of the SIN3-HDAC complex in transcriptional repression is conserved across virtually all eukaryotes (20). Circadian cycles of histone 3 acetylation have been observed at the promoters of clock genes in extraordinarily diverse organisms, including mammals (21, 25–27), insects (28), plants (29), and fungi (30). Thus, it is conceivable that the role of the SIN3-HDAC complex in circadian negative feedback dates

back to the evolutionary origins of eukaryotic circadian clocks.

References and Notes

1. J. S. Takahashi, H. K. Hong, C. H. Ko, E. L. McDearmon, *Nat. Rev. Genet.* **9**, 764 (2008).
2. U. Schibler, J. Ripperger, S. A. Brown, *J. Biol. Rhythms* **18**, 250 (2003).
3. K. A. Lamia, K. F. Storch, C. J. Weitz, *Proc. Natl. Acad. Sci. U.S.A.* **105**, 15172 (2008).
4. K. F. Storch *et al.*, *Cell* **130**, 730 (2007).
5. S. A. Brown *et al.*, *Science* **308**, 693 (2005).
6. C. Lee, J. P. Etchegaray, F. R. Cagampang, A. S. Loudon, S. M. Reppert, *Cell* **107**, 855 (2001).
7. R. Chen *et al.*, *Mol. Cell* **36**, 417 (2009).
8. A. M. Sangoram *et al.*, *Neuron* **21**, 1101 (1998).
9. K. Kume *et al.*, *Cell* **98**, 193 (1999).
10. E. A. Griffin Jr., D. Staknis, C. J. Weitz, *Science* **286**, 768 (1999).
11. S. M. Siepkka *et al.*, *Cell* **129**, 1011 (2007).
12. S. I. Godinho *et al.*, *Science* **316**, 897 (2007).
13. Materials and methods are available as supporting material on Science Online.
14. Y. Nakatani, V. Ogrzyzko, *Methods Enzymol.* **370**, 430 (2003).
15. K. Padmanabhan, M. S. Robles, C. J. Weitz, unpublished observations.
16. Y. Shav-Tal, D. Zipori, *FEBS Lett.* **531**, 109 (2002).
17. M. Mathur, P. W. Tucker, H. H. Samuels, *Mol. Cell. Biol.* **21**, 2298 (2001).
18. M. S. Robles, C. Boyault, D. Knutti, K. Padmanabhan, C. J. Weitz, *Science* **327**, 463 (2010).
19. X. Dong, J. Sweet, J. R. Challis, T. Brown, S. J. Lye, *Mol. Cell. Biol.* **27**, 4863 (2007).
20. A. Grzenda, G. Lomber, J. S. Zhang, R. Urrutia, *Biochim. Biophys. Acta* **1789**, 443 (2009).

21. J. A. Ripperger, U. Schibler, *Nat. Genet.* **38**, 369 (2006).
22. K. Bae *et al.*, *Neuron* **30**, 525 (2001).
23. S. E. Rundlett *et al.*, *Proc. Natl. Acad. Sci. U.S.A.* **93**, 14503 (1996).
24. Y. Nakahata *et al.*, *Cell* **134**, 329 (2008).
25. J. P. Etchegaray, C. Lee, P. A. Wade, S. M. Reppert, *Nature* **421**, 177 (2003).
26. A. M. Curtis *et al.*, *J. Biol. Chem.* **279**, 7091 (2004).
27. Y. Naruse *et al.*, *Mol. Cell. Biol.* **24**, 6278 (2004).
28. P. Taylor, P. E. Hardin, *Mol. Cell. Biol.* **28**, 4642 (2008).
29. M. Perales, P. Más, *Plant Cell* **19**, 2111 (2007).
30. W. J. Belden, J. J. Loros, J. C. Dunlap, *Mol. Cell* **25**, 587 (2007).

Acknowledgments: We thank M. Liu for technical assistance, P. Nakatani (Dana Farber Cancer Institute) for the FH tag, D. Weaver and S. Reppert (University of Massachusetts) for *Per1*^{-/-}/*Per2*^{-/-} mice, N. Copeland (Institute of Molecular and Cell Biology, Singapore) for reagents, and Y. Kurihara (Yokohama National University) for PSF plasmid. This work was supported by the G. Harold and Leila Y. Mathers Charitable Foundation (C.J.W.), NIH Training Grant in Fundamental Neurobiology fellowship (H.A.D.), an Edward R. and Anne G. Lefler Center fellowship (M.S.R.), and a Swiss National Science Foundation fellowship (D.K.).

Supporting Online Material

www.sciencemag.org/cgi/content/full/332/6036/1436/DC1
Materials and Methods
SOM Text
Figs. S1 to S7
References

20 August 2010; accepted 25 March 2011
10.1126/science.1196766

Direct Ubiquitination of Pattern Recognition Receptor FLS2 Attenuates Plant Innate Immunity

Dongping Lu,^{1,3} Wenwei Lin,^{2,3,4} Xiquan Gao,^{1,3} Shujing Wu,^{2,3} Cheng Cheng,^{1,3} Julian Avila,¹ Antje Heese,⁵ Timothy P. Devarenne,¹ Ping He,^{1,3*} Libo Shan^{2,3*}

Innate immune responses are triggered by the activation of pattern-recognition receptors (PRRs). The *Arabidopsis* PRR FLAGELLIN-SENSING 2 (FLS2) senses bacterial flagellin and initiates immune signaling through association with BAK1. The molecular mechanisms underlying the attenuation of FLS2 activation are largely unknown. We report that flagellin induces recruitment of two closely related U-box E3 ubiquitin ligases, PUB12 and PUB13, to FLS2 receptor complex in *Arabidopsis*. BAK1 phosphorylates PUB12 and PUB13 and is required for FLS2-PUB12/13 association. PUB12 and PUB13 polyubiquitinate FLS2 and promote flagellin-induced FLS2 degradation, and the *pub12* and *pub13* mutants displayed elevated immune responses to flagellin treatment. Our study has revealed a unique regulatory circuit of direct ubiquitination and turnover of FLS2 by BAK1-mediated phosphorylation and recruitment of specific E3 ligases for attenuation of immune signaling.

Plants and animals rely on innate immunity to prevent infections by detection of pathogen- or microbe-associated molecular patterns (PAMPs/MAMPs) through pattern-recognition receptors (PRRs) (1–4). *Arabidopsis* FLAGELLIN-SENSING 2 (FLS2), a plasma membrane-localized leucine-rich repeat receptor-like kinase (LRR-RLK), is the receptor for bacterial flagellin (5).

Upon flagellin perception, FLS2 associates instantaneously with another LRR-RLK, termed BAK1, which appears to function as a signaling partner of the growth hormone brassinolide receptor BRI1 and multiple PRRs (6–10). BIK1, a receptor-like cytoplasmic kinase in the FLS2/BAK1 complex, is rapidly phosphorylated upon flagellin perception (11, 12). Ligand-induced FLS2 en-

doytosis has also been suggested to be coupled with the activation of flagellin signaling (13). Similar to PRR activation, down-regulation of PRR signaling is crucial for preventing excessive or prolonged activation of immune responses that would be detrimental to the hosts. Far less understood is how the innate immune responses are attenuated after the PRR activation.

To identify components in MAMP signaling, we performed a yeast two-hybrid screen using the BAK1 kinase domain as bait. One of the interactors isolated encodes the C terminus of *Arabidopsis* PUB13 (At3g46510) (figs. S1 and S2A and table S1) (14). PUB13 is a typical plant U-box (PUB) E3 ubiquitin ligase with a U-box N-terminal domain (UND), a U-box domain, and a C-terminal ARMADILLO (ARM) repeat domain (fig. S1) (15, 16). To test whether full-length PUB13 and BAK1 interact in vivo, we performed a co-immunoprecipitation (Co-IP) assay after protoplast transient transfection. FLAG

¹Department of Biochemistry and Biophysics, Texas A&M University, College Station, TX 77843, USA. ²Department of Plant Pathology and Microbiology, Texas A&M University, College Station, TX 77843, USA. ³Institute for Plant Genomics and Biotechnology, Texas A&M University, College Station, TX 77843, USA. ⁴Key Laboratory of Biopesticide and Chemical Biology, Ministry of Education, Fujian Agriculture and Forestry University, Fuzhou 350002, China. ⁵Department of Biochemistry, University of Missouri–Columbia, Columbia, MO 65211, USA.

*To whom correspondence should be addressed. E-mail: lshan@tamu.edu (L.S.); pinghe@tamu.edu (P.H.)

epitope-tagged PUB13 co-immunoprecipitated hemagglutinin (HA) epitope-tagged BAK1 independent of flg22, a 22-amino acid peptide of flagellin (Fig. 1A). The interaction between FLS2 and PUB13 was barely detectable in the absence of flg22 treatment; however, PUB13 strongly associated with FLS2 upon flg22 stimulation (Fig. 1B). Deletion analysis indicated that the ARM domain of PUB13 was sufficient to associate with FLS2 (fig. S2B). PUB12, the closest homolog of PUB13, but not PUB29, also associated with FLS2 upon flg22 stimulation (fig. S2C). The association of FLS2 with PUB13 was further confirmed in transgenic plants expressing FLAG-tagged *PUB13* under the control of its native promoter (*pPUB13::PUB13-FLAG*) by using an antibody to FLS2 (Fig. 1C).

Because flg22 induces the association of FLS2 with both BAK1 and PUB12/13, we tested whether flg22-induced FLS2-PUB12/13 association required BAK1. flg22-mediated FLS2-PUB13 (Fig. 1D) or FLS2-PUB12 (fig. S2D) association was not detectable in the *bak1-4* mutant plants, indicating that flg22-induced FLS2-PUB12/13 complex formation requires BAK1. However, the interaction of BAK1 and PUB12 does not require FLS2 (fig. S2E), which is consistent with the observation that BAK1 constitutively interacts with PUB12 and PUB13 in the absence of ligand (Fig. 1A and fig. S2, A and E). Similar to the instantaneous association of FLS2 and BAK1, FLS2-PUB13 association was detected within 30 s upon flg22 stimulation (Fig. 1E). Together, the results suggest that BAK1, PUB12, and PUB13 probably exist as a complex that is rapidly recruited to FLS2 receptor upon flg22 stimulation (fig. S2F).

BAK1 directly phosphorylated PUB12 and PUB13 (Fig. 2A). The phosphorylation depended on the kinase activity of BAK1 because a BAK1 kinase mutant (BAK1Km) was unable to phos-

phorylate PUB12 or PUB13 (Fig. 2A). BIK1, an FLS2/BAK1-associated cytosolic kinase, did not phosphorylate PUB12 or PUB13 (fig. S3A). However, BIK1 enhanced the ability of BAK1 to phosphorylate PUB13 (fig. S3A). Consistent with our published data that BIK1 phosphorylates BAK1 (11), it is likely that phosphorylation of BAK1 by BIK1 potentiates BAK1's activity to phosphorylate PUB12 and PUB13. To further examine whether flg22 could enhance BAK1-dependent phosphorylation of PUB13, we performed an immunocomplex kinase assay with flg22-treated protoplasts expressing full-length BAK1. The immunoprecipitated BAK1, but not kinase-inactive BAK1Km, phosphorylated PUB13 (Fig. 2B). The phosphorylation of PUB13 was further enhanced upon flg22 treatment, depending on its receptor FLS2 (Fig. 2B). These data suggest that PUB12 and PUB13 are substrates of BAK1, and that flg22 perception stimulates BAK1 phosphorylation of PUB12 and PUB13, which is probably further potentiated by BIK1 (fig. S3C). To examine the biological significance of PUB12 and PUB13 phosphorylation, we tested whether phosphorylation is required for the flg22-induced FLS2-PUB12/13 association. We found that the flg22-induced FLS2-PUB13 or FLS2-PUB12 association was blocked by the kinase inhibitor K252a (Fig. 2C and fig. S3B). These results support the importance of phosphorylation events in FLS2-PUB12/13 association (fig. S3C).

An *in vitro* ubiquitination assay with glutathione *S*-transferase (GST)-PUB12/13 fusion proteins in the presence of recombinant AtUBA1 (E1), AtUBC8 (E2), adenosine 5'-triphosphate (ATP), and FLAG-tagged ubiquitin (Ub) demonstrates that PUB12 and PUB13 possess auto-ubiquitination activity as detected with either antibody to FLAG or antibody to GST (fig. S4A). Both PUB12 and PUB13 polyubiquitinated the

cytosolic domain of FLS2, which was evidenced by detection of a ladder-like smear with high-molecular-weight proteins (Fig. 3A). Eliminating E1, E2, PUB13, Ub, or ATP from the reaction blocked the ladder formation for FLS2 (fig. S4B). Mutation of the conserved cysteine or tryptophan residue to alanine (C262A or W289A) within the U-box motif of PUB13 abolished its Ub ligase activity on FLS2 (Fig. 3B) (17). The specificity of FLS2 ubiquitination by PUB12 and PUB13 was further substantiated by the observation that several U-box E3 ubiquitin ligases, including PUB14 and PUB29, did not ubiquitinate FLS2 (fig. S4C). PUB12 and PUB13 did not ubiquitinate the cytosolic domain of BAK1 or BIK1 (Fig. 3C). Thus, PUB12 and PUB13 specifically ubiquitinate the PRR FLS2 but not the signaling components BAK1 or BIK1 (fig. S5C).

It has been shown that flg22 induces FLS2 translocation into intracellular vesicles, which is followed by degradation of FLS2 (13). FLS2 possesses a PEST-like motif in the C terminus, which is required for FLS2 endocytosis. In addition, a potential phosphorylation site, Thr⁸⁶⁷, is essential for FLS2 internalization and signaling (13). However, neither the T867V nor a PEST mutant P1076A abolished FLS2 ubiquitination by PUB13 or PUB12 (fig. S5A), suggesting that FLS2 ubiquitination and internalization are probably uncoupled. It has been reported that the ubiquitination of FLS2 by a bacterial effector AvrPtoB is also independent of its PEST domain (18). An FLS2 kinase inactive mutant K898M also did not affect FLS2 ubiquitination by PUB13 (fig. S5B), indicating that FLS2 kinase activity is not required for its ubiquitination. This is consistent with our data that PUB12 and PUB13 are phosphorylated by BAK1 and that phosphorylation is required for flg22-induced FLS2-PUB12/13 association. Our data also sug-

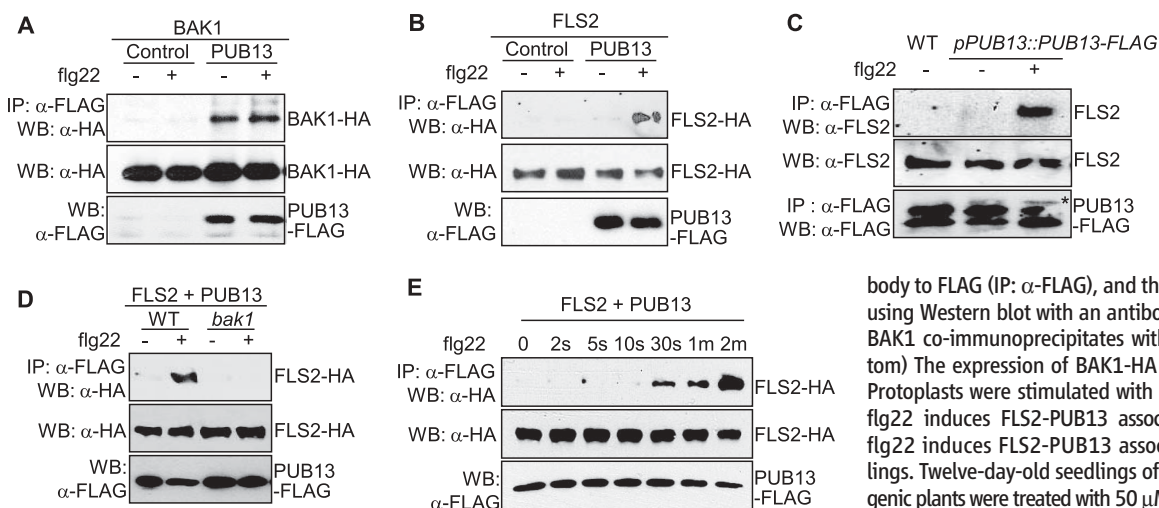


Fig. 1. Flagellin induces BAK1-dependent FLS2-PUB13 complex association. (A) BAK1 interacts with PUB13 in a Co-IP assay. Protoplasts were co-expressed with BAK1-HA and PUB13-FLAG or a control vector. The Co-IP was carried out with an antibody to FLAG (IP: α-FLAG), and the proteins were analyzed by using Western blot with an antibody to HA (WB: α-HA). (Top) BAK1 co-immunoprecipitates with PUB13. (Middle and bottom) The expression of BAK1-HA and PUB13-FLAG proteins. Protoplasts were stimulated with 1 μM flg22 for 10 min. (B) flg22 induces FLS2-PUB13 association in protoplasts. (C) flg22 induces FLS2-PUB13 association in *Arabidopsis* seedlings. Twelve-day-old seedlings of *pPUB13::PUB13-FLAG* transgenic plants were treated with 50 μM MG132 for 1 hour before H₂O or 1 μM flg22 treatment for 10 min. Asterisk indicates

the specific band of PUB13-FLAG in *pPUB13::PUB13-FLAG* transgenic plants. (D) flg22-induced FLS2-PUB13 association depends on BAK1. (E) flg22 stimulates rapid association of FLS2-PUB13. The above experiments were repeated at least three times with similar results.

gest that FLS2 ubiquitination is distinct from mammalian receptor tyrosine kinase (RTK), in which a kinase-defective mutant blocked RTK ubiquitination (19).

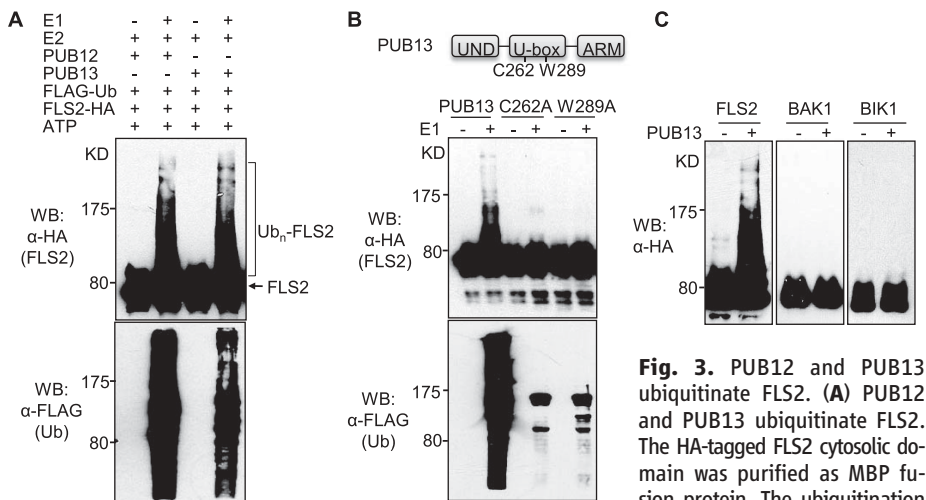
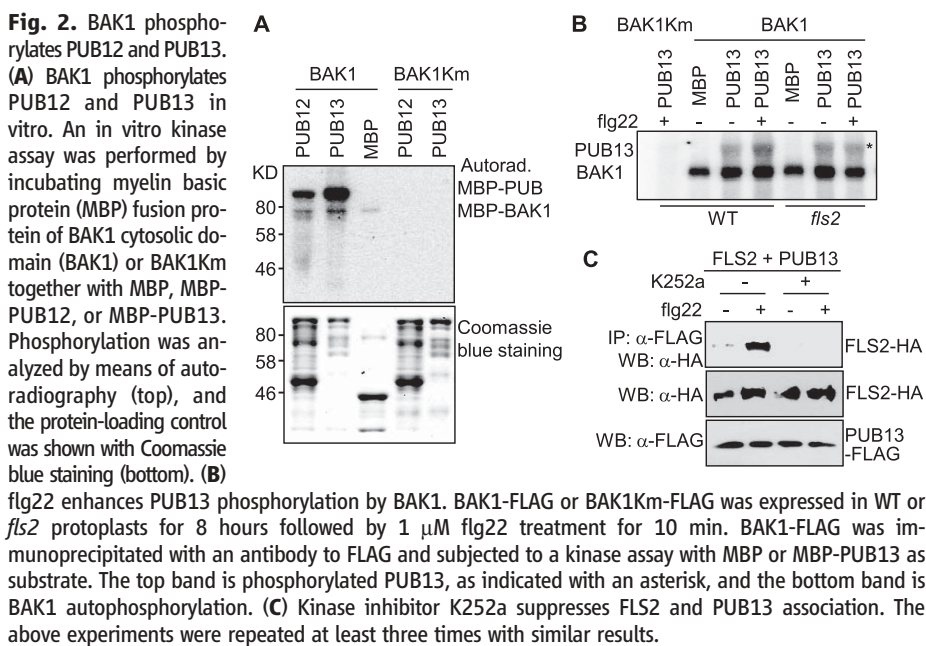
To further demonstrate the biological function of PUB12 and PUB13 in plant innate immunity, we isolated their transferred DNA (T-DNA) insertional mutants. Reverse transcriptase-polymerase chain reaction analysis indicated that *pub12-1* (SAIL_35_G10) displayed a slight reduction of transcript, whereas *pub12-2* (WiscDsLox497_01) showed a pronounced transcript reduction and so was selected for further analyses (fig. S6). The *pub13* mutant (SALK_093164) is a null mutant with undetectable transcript (fig. S6). We examined the immune responses in wild-type (WT), *pub12-2*, and *pub13* mutants. Flg22-

induced FLS2/BAK1 association (fig. S7A) and BIK1 phosphorylation (fig. S7B) occurred similarly in *pub12-2* and *pub13* mutants and in WT plants, suggesting that PUB12 and PUB13 are not required for flg22 perception by FLS2. When treated with flg22, *pub12-2* and *pub13* mutants accumulated two- to threefold more H₂O₂ production than WT plants (Fig. 4A). Similarly, the *pub12-2* and *pub13* mutants showed more callose deposits than WT plants (Fig. 4B and fig. S6C). The complementation lines of the *pub13* mutants transformed with a *pPUB13::PUB13-FLAG* construct displayed a similar level of H₂O₂ production (fig. S8A) and callose deposition (fig. S8, B and C) as the WT plants upon flg22 stimulation. Compared with WT plants, the induction of immune responsive genes *WRKY30*, *AP2* (*At3g23230*), and

FRK1 was further enhanced in the *pub12-2* and *pub13* mutants upon flg22 treatment (Fig. 4C). The basal expression level of these genes was comparable in WT and *pub12-2* or *pub13* mutants, suggesting that *pub12-2* and *pub13* mutants are not constitutively expressing immunity-related genes. Together, these data indicate that flg22-mediated responses are potentiated in the *pub12* and *pub13* mutants, and that *PUB12* and *PUB13* play a negative role in FLS2 signaling.

We performed pathogen infection assays with WT and *pub* mutants. Neither *pub12-2* nor *pub13* mutants showed substantially altered disease symptoms or bacterial multiplication after *Pseudomonas syringae* pv. *tomato* DC3000 infection as compared with WT plants (fig. S9A). To reveal potentially functional redundancy, we generated a *pub12/13* double mutant. The *pub12/13* mutant did not display any obvious growth defects under normal growth conditions, which is consistent with that *pub12-2* and *pub13* mutants did not constitutively activate immunity-related genes. Alternatively, additional components might play redundant functions with PUB12 and PUB13 in the control of detrimental effect of constitutively active defense systems. The *pub12/13* mutant was more resistant to DC3000 infection than WT plants. Three days after infection, the bacterial population in the *pub12/13* mutant was about 10-fold lower than that in WT plants (Fig. 4D). The disease symptoms were also less severe in the *pub12/13* mutant as compared with WT plants 6 days after infection (fig. S9B). Similarly, the *pub12/13* mutants were also more resistant to *P. syringae maculicola* ES4326 infection, as measured by bacterial growth and disease symptoms (Fig. 4D and fig. S9B).

Ubiquitination could lead to protein degradation or in some cases modulation of the activity or localization of a protein target. We examined FLS2 protein level in WT and the *pub12/13* mutant with an antibody to FLS2. We repeatedly observed an apparent reduction of FLS2 protein level within 30 min after flg22 treatment in WT plants (Fig. 4E), which is consistent with the report of ligand-induced FLS2 endocytosis/degradation (13). This degradation was diminished by treatment with MG132, an inhibitor of proteasome-mediated degradation (Fig. 4E), suggesting the involvement of the 26S proteasome in FLS2 degradation. FLS2 protein level was not significantly reduced in the *pub12/13* mutant treated with flg22 (Fig. 4E and fig. S10A), suggesting the involvement of *PUB12* and *PUB13* in flg22-mediated FLS2 degradation. Similar to the *pub12/13* mutant, the reduced FLS2 level triggered by flg22 was not evident in the *bak1-4* mutant (fig. S10B). This is consistent with the FLS2-PUB12/13 association being dependent on BAK1 (Fig. 1D and fig. S2D). We further developed an in vivo ubiquitination assay with protoplast transient transfection of FLAG-tagged UBQ10. The treatment of flg22 enhanced FLS2 ubiquitination, as detected with an antibody to FLS2 (fig. S10C). The flg22-mediated FLS2



of FLS2 was detected by an antibody to HA. The overall ubiquitination was detected by an antibody to FLAG. (B) C262 and W289 are required for PUB13 E3 ligase activity. (C) PUB13 ubiquitinates FLS2 but not BAK1 or BIK1. The above experiments were repeated three times with similar results.

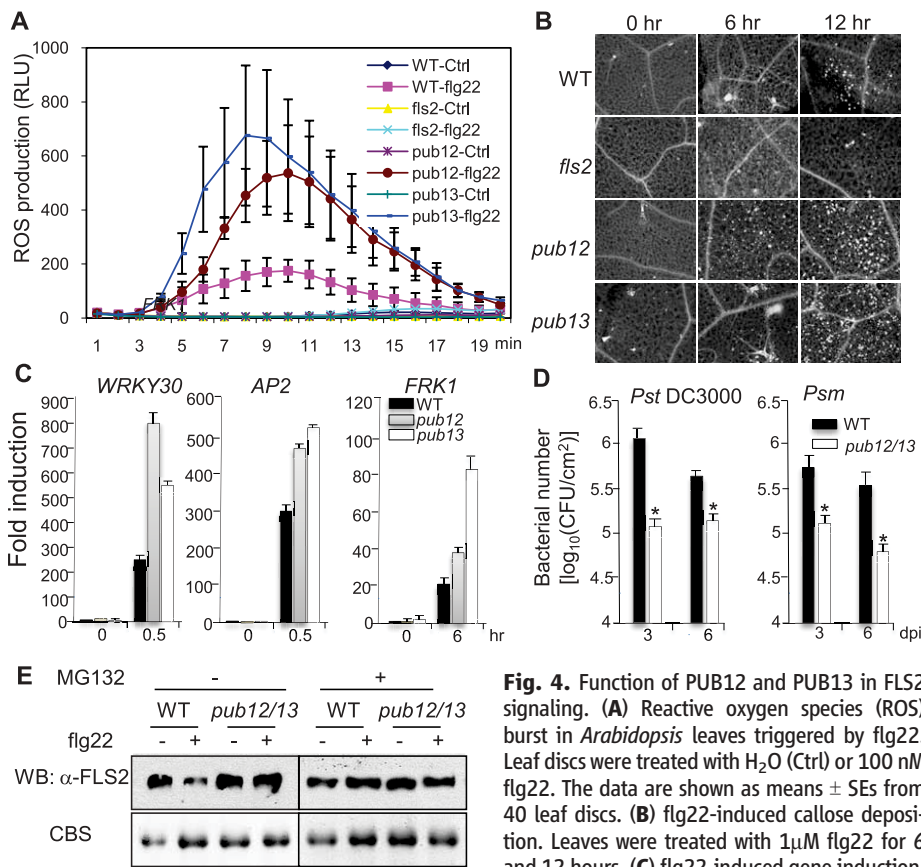


Fig. 4. Function of PUB12 and PUB13 in FLS2 signaling. **(A)** Reactive oxygen species (ROS) burst in *Arabidopsis* leaves triggered by flg22. Leaf discs were treated with H₂O (Ctrl) or 100 nM flg22. The data are shown as means ± SEs from 40 leaf discs. **(B)** flg22-induced callose deposition. Leaves were treated with 1 μM flg22 for 6 and 12 hours. **(C)** flg22-induced gene induction. **(D)** The bacterial growth assay of DC3000 and *Psm*. Four-week-old *Arabidopsis* plants were inoculated with bacteria at a concentration of 5 × 10⁵ colony-forming units/ml. The data are shown as means ± SEs from three replicates. Asterisk indicates a significant difference with *P* < 0.05 when compared with data from WT plants. **(E)** PUB12 and PUB13 promote FLS2 degradation. Twelve-day-old seedlings were treated with or without 50 μM MG132 for 1 hour before 1 μM flg22 treatment for 0.5 hours. The equal protein loading was shown by means of Coomassie blue staining (CBS) for RuBisCo (bottom). The above experiments were repeated three to four times with similar results.

ubiquitination was reduced in the *pub12/13* mutant (fig. S10C), which substantiates the role of PUB12 and PUB13 in the ubiquitination of endogenous FLS2 (fig. S11).

Ubiquitination has been implicated in plant innate immunity (20, 21). Two *Avr9/Cf9* rapidly elicited *PUB* genes are required for programmed cell death and defense in tobacco, tomato, and *Arabidopsis* (22, 23). Three closely related *Arabidopsis* PUBs—PUB22, PUB23, and PUB24—negatively regulate flagellin signaling (24). Rice SPL11, one of the closest homologs to PUB12 and PUB13, is a negative regulator of plant cell death (25). Similarly, a rice RING finger E3 ligase XB3 could be phosphorylated by PRR XA21, mediating bacterial resistance (26). However, the modes of action of these E3 ligases from upstream activators to downstream substrates are largely unknown. Identification of PUB12 and PUB13 as negative regulators of flagellin signaling through direct ubiquitination of FLS2 not only contributes to the general understanding of innate immune signaling but also improves

our ability for genetic manipulation of disease-resistant crop plants without deleterious side effects.

Ubiquitination-mediated Toll-like receptor (TLR) degradation serves as one of the mechanisms to down-regulate TLR signaling (27). Triad 3A, a RING finger E3 ligase mediating ubiquitination and proteolytic degradation of TLR4 and TLR9, appears to be analogous to PUB12 and PUB13 in *Arabidopsis* FLS2 signaling (27). However, the regulation and activation of TLR ubiquitination remain unknown. The mechanism of activating FLS2 ubiquitination is also unique and distinct from RTK signaling (fig. S11). The ubiquitination of RTKs is regulated by ligand-induced RTK phosphorylation (28). It appears that FLS2 phosphorylation is not required for its ubiquitination (fig. S5, A and B). Instead, phosphorylation appears to be required for flg22-induced FLS2–PUB12/13 association (Fig. 2C and fig. S3B). It is plausible that phosphorylation of PUB12 and PUB13 promotes their association with FLS2 *in vivo* (fig. S11). Ubiquitination only occurs on FLS2 and not

BAK1, a common signaling partner of multiple membrane receptors involved in immunity and development. This suggests a mechanism of how the specificity of the signal output is determined for a shared signaling component.

References and Notes

- O. Takeuchi, S. Akira, *Cell* **140**, 805 (2010).
- T. Boller, G. Felix, *Annu. Rev. Plant Biol.* **60**, 379 (2009).
- J. D. Jones, J. L. Dangl, *Nature* **444**, 323 (2006).
- P. N. Dodds, J. P. Rathjen, *Nat. Rev. Genet.* **11**, 539 (2010).
- L. Gómez-Gómez, T. Boller, *Mol. Cell* **5**, 1003 (2000).
- D. Chinchilla *et al.*, *Nature* **448**, 497 (2007).
- A. Heese *et al.*, *Proc. Natl. Acad. Sci. U.S.A.* **104**, 12217 (2007).
- J. Li *et al.*, *Cell* **110**, 213 (2002).
- K. H. Nam, J. Li, *Cell* **110**, 203 (2002).
- B. Schulze *et al.*, *J. Biol. Chem.* **285**, 9444 (2010).
- D. Lu *et al.*, *Proc. Natl. Acad. Sci. U.S.A.* **107**, 496 (2010).
- J. Zhang *et al.*, *Cell Host Microbe* **7**, 290 (2010).
- S. Robatzek, D. Chinchilla, T. Boller, *Genes Dev.* **20**, 537 (2006).
- Materials and methods are available on Science Online.
- D. Yee, D. R. Goring, *J. Exp. Bot.* **60**, 1109 (2009).
- C. Azevedo, M. J. Santos-Rosa, K. Shirasu, *Trends Plant Sci.* **6**, 354 (2001).
- Single-letter abbreviations for the amino acid residues are as follows: A, Ala; C, Cys; D, Asp; E, Glu; F, Phe; G, Gly; H, His; I, Ile; K, Lys; L, Leu; M, Met; N, Asn; P, Pro; Q, Gln; R, Arg; S, Ser; T, Thr; V, Val; W, Trp; and Y, Tyr. In the mutants, other amino acids were substituted at certain locations; for example, H134R indicates that histidine at position 134 was replaced by arginine.
- V. Göhre *et al.*, *Curr. Biol.* **18**, 1824 (2008).
- G. Levkowitz *et al.*, *Mol. Cell* **4**, 1029 (1999).
- A. Craig, R. Ewan, J. Mesmar, V. Gudipati, A. Sadanandom, *J. Exp. Bot.* **60**, 1123 (2009).
- M. Trujillo, K. Shirasu, *Curr. Opin. Plant Biol.* **13**, 402 (2010).
- C. W. Yang *et al.*, *Plant Cell* **18**, 1084 (2006).
- R. González-Lamothe *et al.*, *Plant Cell* **18**, 1067 (2006).
- M. Trujillo, K. Ichimura, C. Casais, K. Shirasu, *Curr. Biol.* **18**, 1396 (2008).
- L. R. Zeng *et al.*, *Plant Cell* **16**, 2795 (2004).
- Y. S. Wang *et al.*, *Plant Cell* **18**, 3635 (2006).
- T. H. Chuang, R. J. Ulevitch, *Nat. Immunol.* **5**, 495 (2004).
- M. A. Lemmon, J. Schlessinger, *Cell* **141**, 1117 (2010).

Supporting Online Material

www.sciencemag.org/cgi/content/full/332/6036/1439/DC1
 Materials and Methods
 Figs. S1 to S11
 Table S1
 References (29–33)

28 February 2011; accepted 29 April 2011
 10.1126/science.1204903

Materials and Methods

Plant material and growth conditions

Wild-type (Col-0), *fls2*, *bak1-4*, *pub12-1*, *pub12-2*, *pub13* and *pub12/pub13* mutant *Arabidopsis* plants were grown in a growth room at 23°C, 60% relative humidity, 75 μ E light with a 12 hr photoperiod for 30 days before protoplast isolation or bacterial inoculation. The *pub12-1* (SAIL_35_G10), *pub12-2* (WiscDsLox497_01), and *pub13* (SALK_093164) mutants were obtained from Arabidopsis Biological Resource Center (ABRC), and confirmed by PCR and RT-PCR analyses. The *pub12/pub13* double mutant was generated by the genetic cross between *pub12-2* and *pub13*, and confirmed by PCR and RT-PCR analyses. Seedlings were grown on ½MS plates with 0.5% sucrose and 0.9% agar at 23°C and 75 μ E light with a 12 hr photoperiod for 12 days. Seedlings were transferred to 2 ml H₂O in the 6-well tissue culture plates one day before flg22 treatment for RT-PCR analysis or protein extraction. All experiments were repeated 3-4 times with reproducible results. Typical results with statistical analyses are shown.

cDNA library construction and yeast two-hybrid screen

Total RNA was isolated from 4-week-old *Arabidopsis* plants inoculated with DC3000 *hrcC* at the concentration of 10⁸ cfu/ml for 2 hr and 6 hr. The mRNA was obtained with PolyAtract mRNA isolation system (Promega). The first- and second-strand cDNA synthesis was performed by standard molecular cloning protocols with an oligo (dT)-XhoI primer and EcoRI adaptor. The cDNA was XhoI digested, size-fractionated, and ligated with EcoRI/XhoI digested modified pGADT7 vector (Clontech). About 100,000 clones were screened for interaction with the BAK1 kinase domain in a DNA-binding domain fusion vector pBridge (Clontech) in the medium SD-T-L-H-A. The positive clones were further confirmed with additional yeast two-hybrid assays with empty vector controls, and the gene identity was revealed by sequencing and BLAST search.

Plasmid constructs, protoplast transient assay, and generation of transgenic plants.

Arabidopsis *BAK1*, *FLS2*, and *BIK1* constructs were reported previously (11). *PUB12*, *PUB13*, *PUB14* and *PUB29* genes were amplified by PCR from Col-0 cDNA, and introduced into a plant expression vector with an HA or FLAG epitope-tag at the C terminus. UBQ10 was cloned into a plant expression vector with an FLAG epitope-tag at the N terminus. Based on the cDNA

sequences of our PUB12 clones and the expressed sequence tag (EST) database, the C terminus of the protein was apparently mis-annotated in the database of The Arabidopsis Information Resource (TAIR). Figure S1 shows the correct sequences of PUB12 with 65% identity and 79% similarity with PUB13 at the amino acid level. PUB13 and FLS2 point mutations were generated by a site-directed mutagenesis kit (Stratagene). The primer sequences for different PUBs, PUB13 and FLS2 point mutations and truncations are listed in Supplemental Experimental Procedures. Full-length PUBs, cytosolic domain or kinase domain of BAK1 and FLS2 were sub-cloned into a modified GST or MBP fusion protein expression vector pGEX4T-1 (Pharmacia) or pMAL-C2 (New England Biolabs) with BamHI/NcoI and StuI digestion. Protoplast transient assay was carried out as described (29). For Co-IP assays, 1 ml protoplasts were transfected with 200 µg of DNA. The *PUB13* transgenic plants in Col-0 and *pub13* mutant were generated by *Agrobacterium*-mediated transformation with the *PUB13* cDNA in pCB302 vector under the control of its native promoter with an FLAG tag. The *PUB13* promoter was amplified from genomic DNA of Col-0 with primers 5'-CCGCTCGAGGAGCTCACTAGTTTCTTCATTGAGACCAATATC-3' and 5'-CATGCCATGGTGAATTGATTCTTCTCTG-3'.

Co-immunoprecipitation, *in vitro* phosphorylation and immunocomplex kinase assays.

For transgenic plants, twelve-day-old seedlings or leaves of 4-week-old soil-grown plants carrying the *pPUB13::PUB13-FLAG* transgene were ground with 1 ml of extraction buffer (10 mM HEPES, pH7.5, 100 mM NaCl, 1 mM EDTA, 10% Glycerol, 0.5% Triton X-100 and protease inhibitor cocktail from Roche). For protoplasts, samples were lysed with 0.5 ml of extraction buffer. After vortexing vigorously for 30 sec, the samples were centrifuged at 13,000 rpm for 10 min at 4°C. For the co-IP assay, the supernatant was incubated with an anti-HA or anti-FLAG antibody for 2 hr, and then protein-G-agarose beads for another 2 hr at 4°C with gentle shaking. The immunoprecipitated proteins were analyzed by Western blot with an anti-HA, -FLAG or -FLS2 antibody. The protein bands with appropriate molecular weight are shown.

Expression of the GST and MBP fusion proteins and affinity purification were performed as standard protocol, and *in vitro* phosphorylation and immunocomplex kinase assays were carried out as described (11).

***In vitro* ubiquitination assay**

The *in vitro* ubiquitination assays were performed as described with some modifications (30). The reactions contain 500 ng of substrate protein, 250 ng of purified His₆-E1 (AtUBA1), 500 ng of purified His₆-E2 (AtUBC8), 1.25 µg of FLAG tagged ubiquitin (Boston Biochem) and 1 µg of purified GST-PUB in the ubiquitination buffer (0.1 M Tris-HCl pH 7.5, 25 mM MgCl₂, 2.5 mM dithiothreitol, 10 mM ATP) to a final volume of 30 µl. The reactions were incubated at 30°C for 2 hr, and then stopped by adding SDS sample buffer and boiled at 100°C for 5 min. The samples were then separated by 7.5% SDS-PAGE and the ubiquitinated substrates were detected by Western blotting analysis.

Measurement of ROS production

ROS burst was determined by a luminol-based assay as described with modifications (31). Four to five leaves of each five-week-old *Arabidopsis* plant were excised into leaf discs of 0.25 cm², following an overnight incubation in 96-well plate with 100 µl of H₂O to eliminate the wounding effect. H₂O was replaced by 100 µl of reaction solution containing 50 µM of luminol and 10 µg/ml of horseradish peroxidase (Sigma) supplemented with 100 nM of flg22. The measurement was conducted immediately after adding the solution with a luminometer (Perkin Elmer, 2030 Multilabel Reader, Victor X3), with a 1 min interval reading time for a period of 20 min. The measurement values for ROS production from 40 leaf discs per treatment were indicated as means of RLU (Relative Light Units). The experiments were repeated four times and similar results were obtained.

Callose deposition

Callose deposition was conducted as described by Wang et al. with modifications (32). Briefly, two to three leaves of 5-week-old Col-0 and *pub* mutant plants were infiltrated with 1 µM of flg22, and leaves were excised 6 and 12 hr after infiltration. Control treatments were infiltrated with H₂O. Excised leaves were immediately cleared in alcoholic lactophenol [95% ethanol: lactophenol (phenol : glycerol : lactic acid : H₂O=1:1:1:1) = 2:1] for overnight. Samples were subsequently rinsed with 50% ethanol and H₂O. Cleared leaves were stained with 0.01% aniline

blue in 0.15 M phosphate buffer (pH = 9.5) and the callose deposits were visualized under a UV filter using a fluorescence microscope. Callose deposits were counted using ImageJ 1.43U software (<http://rsb.info.nih.gov/ij/>). The number of deposits was expressed as the mean of three different leaf areas and analyzed using the general linear model of SAS (SAS Institute, Inc., Cary, NC), with mean separations by least significant difference (LSD). At least three independent experiments were conducted with similar results obtained.

Pathogen infection assays

P. syringae tomato DC3000 and *P. syringae maculicola* ES4326 strains were grown overnight at 28°C in the KB medium with 50 µg/ml rifampicin for DC3000 and 50 µg/ml streptomycin for ES4326. Bacteria were collected, washed and diluted to the desired density with H₂O. Four-week-old *Arabidopsis* leaves were infiltrated with bacteria at a concentration of 5x10⁵ cfu/ml using a needleless syringe. To measure bacterial growth, two leaf discs were ground in 100 µl H₂O and serial dilutions were plated on KB medium with appropriated antibiotic. Bacterial colony forming units (cfu) were counted 2 days after incubation at 28°C. Each data point is shown as triplicates (33).

Primers for construct cloning and point mutations

Primer Name	Sequences
PUB12-BamHI-F	CG GGATCC ATGGCGAAATCAGAGAAACAC
PUB12-SmaI-R	TCCCCCGGGGATTAGGGAGATTTGATCTTCC
PUB13-NcoI-F	CATGCCATGGAGGAAG AGAAAGCTTC
PUB13-StuI-R	GAAGGCCTAGTATCTGCAGCTTCTGTGG
PUB13-ARM-NcoI-F	CATGCCATGGAGCCT CCAAAGCCTCCGAG
PUB13 Promoter-XhoI/SacI/SpeI-F	CCG CTCGAG GAGCTC ACTAGT TTCTTCATTGAGACCAATATC
PUB13 Promoter-NcoI-R	CATGCCATGGTGAATTGATTCTTCTCTG
PUB14-NcoI-F	CATG CC ATGGGATTAACGAATTGTTG
PUB14-StuI-R	GAAGGCCTTGGAACAGTAGTTACTGC
PUB29-BamHI/NcoI-F	CG GGATCC ATGGGGAGAG ATGAAACAG
PUB29-StuI-R	GAAGGCCTAAAAGGCATAATATGAGTAG
PUB13-C262A-F	TGATGATTTT CGCGCTCCGA TTTCGCTG
PUB13-C262A-R	CAGCGAAATCGGAGCGCGAAAATCATCA
PUB13-W289A-F	CATGTATTGA GAAAGCGATA GAAGGTGG
PUB13-W289A-R	CCACCTTCTATCGCTTTCTCAATACATG
UBQ10-BamHI-F	CGGGATCCATGCAGATCT TTGTTAAGAC TCTCACC
UBQ10-StuI-R	AACTGCAGAGGCCTTTAACCACCACGGAGCCTGAGG
FLS2-T867V-F	TTGG AGCAAGCAGTAGATTCATTC AAC
FLS2-T867V-R	GTTGAATGAATCTACTGCTTGCTCCAA
FLS2-K898M-F	GATTGCAGTAATGGTATTGAATCTAAAG
FLS2-K898M-R	CTTTAGATTCAATACCATTACTGCAATC
FLS2-P1076A-F	GACGAAAC AGAGAGCAAC TTCGTTGAAT G
FLS2-P1076A-R	CATTCAACGAAGTTGCTCTCTGTTTCGTC

Primers for RT-PCR analysis

PUB12-F	CAAGCTCCACCTGTTCTTTAAGT
PUB12-R	CCTGGTGTGGAGAGAGATCA
PUB13-F	GATTGCTGCGATTTCTGA
PUB13-R	TTATCATCTCCGTCCTGC

Primers for confirming T-DNA insertions in pub knockout

pub12-2-LP	TAACCACAGCTACCCAAAACG
pub12-2-RP	TAATTTCCCTAATTTGGCCGTG
pub13-LP	AAGAGGTATGGCTCCAGCTTC
pub13-RP	ACGTGCTTTGTTTTGCTATGG

Supplemental data

	1	UND domain																				130
PUB12	MAKSEKHKLA	QTLIDSINEI	ASISDSVTPM	KKHCANLSRR	LSLLLPMLLE	IRDNQESSSE	-VVNALLSVK	QSLHAKDLL	SFVSHVSKIY	LVLERDQVMV	KFQKVTSLLE	QALSIIPYEN	LEISDELKEQ									
PUB13	MEEKASAA	QSLIDVVNEI	AAISDYRITV	KKLCYNLARR	LKLLVPMFEE	IRESNEPISE	DTLKTLMNLK	EAMCSAKDYL	KFCSQGSKIY	LVMEREQVTS	KLMEVSVKLE	QSLSQIPYEE	LDISDEVREQ									
	131	UND domain																				260
PUB12	VELVLVQLRR	SLGKRGGDVY	DDELYKDVLS	LYSGRGSV-M	ESDMVRRVAE	KLQLMTITDL	TQESLALLDM	VSSSGGDDPG	ESFEKMSMVL	KKIKDFVQTY	NPNLDDAPLR	LKSSLPKSRD	DDRDLIP--									
PUB13	VELVLSQFRR	AKGRV--DVS	DDELYEDLQS	LCNKSSDVDA	YQFVLERVAK	KLHLMETPDL	AQESVALHEM	VASSGGD-VG	ENIEEMAMVL	KMIKDFVQTE	DDNGEEQKVG	VNSRSNGQTS	TAASQKIPVI									
	261	U-box																				390
PUB12	PEEFRQ	PISL	ELMTDPVIVS	SGQTYERE	CKKLEGGHLT	CPKTQETLTS	DIMTPNYVLR	SLIAQWCESN	GIEPPKRPNI	SQFSSKASSS	SSAPDDEHNK	IEEELLKLT	QQPEDRRSAA	GEIRLLAKQN								
PUB13	PDDFRQ	PISL	EMMRDPVIVS	SGQTYERTCI	EKKIEGGHST	CPKTQQALTS	TILTPNYVLR	SLIAQWCEAN	DIEPPKPPSS	LRPRKVSSFS	SPA---EANK	IEDLMWRLAY	GNPEDQRSAA	GEIRLLAKRN								
	391	ARM repeats																				520
PUB12	NHNRAVAIAS	GAIPLLVNL	TISNDSRTQE	HAVTSLNL	ICQENKGI	YSSGAVPGIV	HVLQKGSMEA	RENAATLFS	LSVIDENKVT	IGAGAIPLP	VTLLESGSQR	GKKDAATALF	NLCIFQGNKG									
PUB13	ADNRVAIAEA	GAIPLLVGLL	S-TPDSRIQE	HSVTALLNL	ICENNKGAIV	-SAGAIPIGIV	QVLKKSMEA	RENAATLFS	LSVIDENKVT	IGALGAIPLP	VLLNEGTQR	GKKDAATALF	NLCIYQGNKG									
	521	ARM repeats																				650
PUB12	KAVRAGLVPV	LMRLLTEPES	GMVDELSIL	AILSSHPDGK	SEVGAADAVP	VLVDFIRSGS	PRNKENSAV	LVHLCSWNQQ	HLIEAQKGLI	MDLLIEMAEN	GDRGKRKAA	QLLNRFSRFN	DQQKQHSGLG									
PUB13	KAIRAGVIPT	LTRLLETPGS	GMVDEALAIL	AILSSHPGEGK	AIIGSSDAVP	SLVEFIRTGS	PRNRENAAV	LVHLCSGDPQ	HLVEAQKGLL	MGPLIDLGN	GDRGKRKAA	QLLERISRLA	EQQKETAVSQ									
	651	669																				
PUB12	LEDQISLI																					
PUB13	PEEEAEPHP	ESTTEAADT																				

Fig. S1. The alignment of the amino acid sequences of PUB12 and PUB13. The UND domain, U-box and ARM repeats are indicated. The conserved cysteine (C) and tryptophan (W) residues are highlighted in yellow.

Supplemental data

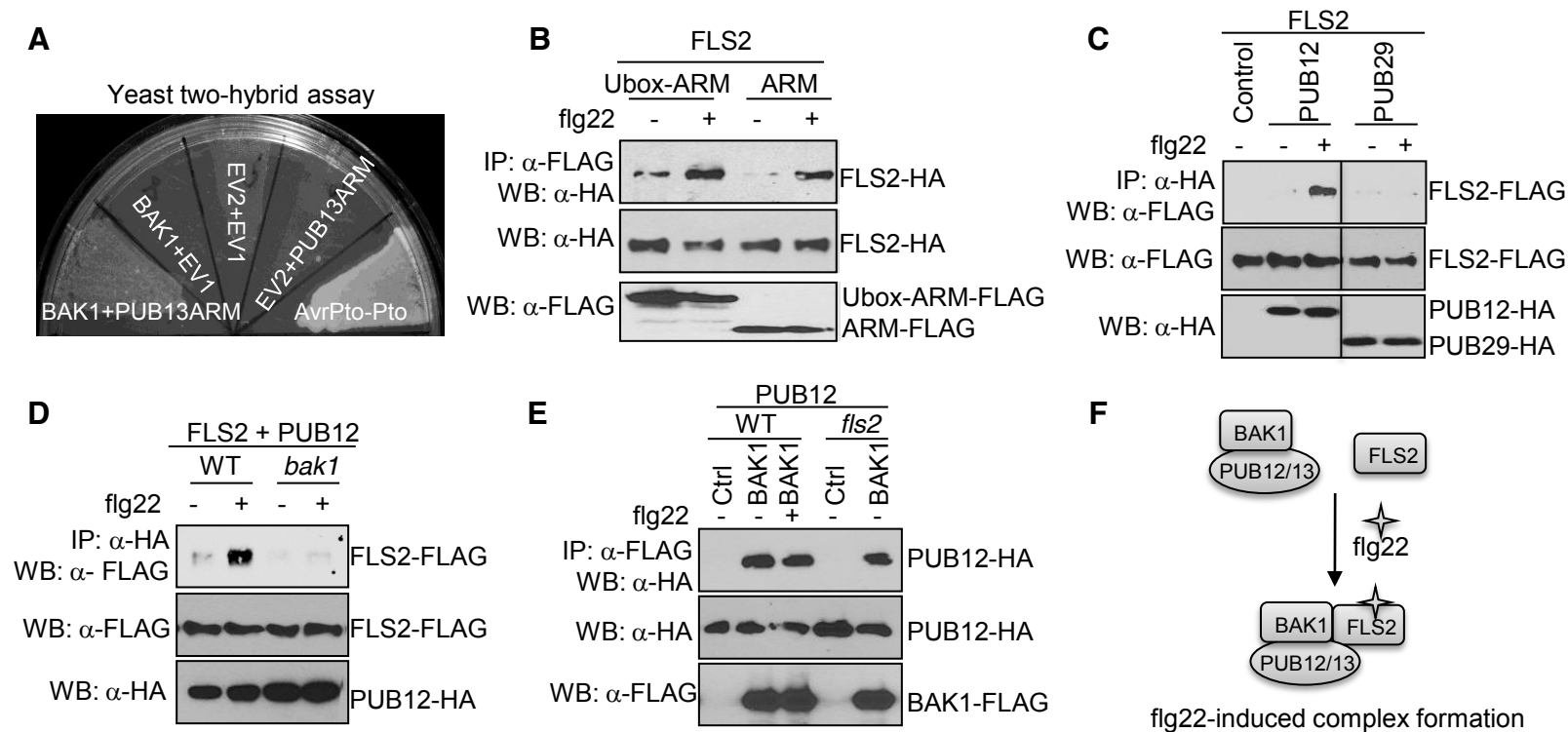


Fig. S2. Association of PUB12/13 with FLS2 and BAK1. (A) BAK1 kinase domain interacts with the PUB13 ARM domain in a yeast two-hybrid assay. EV, empty vector. The interaction of AvrPto and Pto is a positive control. The yeast colonies were grown on a SD-L-T-A-H plate at 30°C for 4 days. (B) The ARM domain of PUB13 is sufficient to associate with FLS2. The Co-IP was carried out with an anti-FLAG antibody (IP: α -FLAG), and the proteins were analyzed using Western blot with an anti-HA antibody (WB: α -HA). The top panel shows that FLS2 co-immunoprecipitates with PUB13 ARM domain or Ubox-ARM domain. The middle and bottom panels show the protein expression of FLS2-HA and FLAG tagged PUB13Ubox-ARM or PUB13ARM. Protoplasts were stimulated with 1 μ M flg22 for 10 min. (C) flg22 induces FLS2-PUB12, not FLS2-PUB29 association. (D) flg22-induced FLS2-PUB12 association depends on BAK1. FLS2-FLAG and PUB12-HA were co-expressed in WT or *bak1-4* mutant protoplasts. (E) BAK1-PUB12 interaction is independent of FLS2. The above experiments were repeated at least three times with similar results. (F) A model of flg22-induced FLS2/BAK1/PUB12/13 complex formation.

Supplemental data

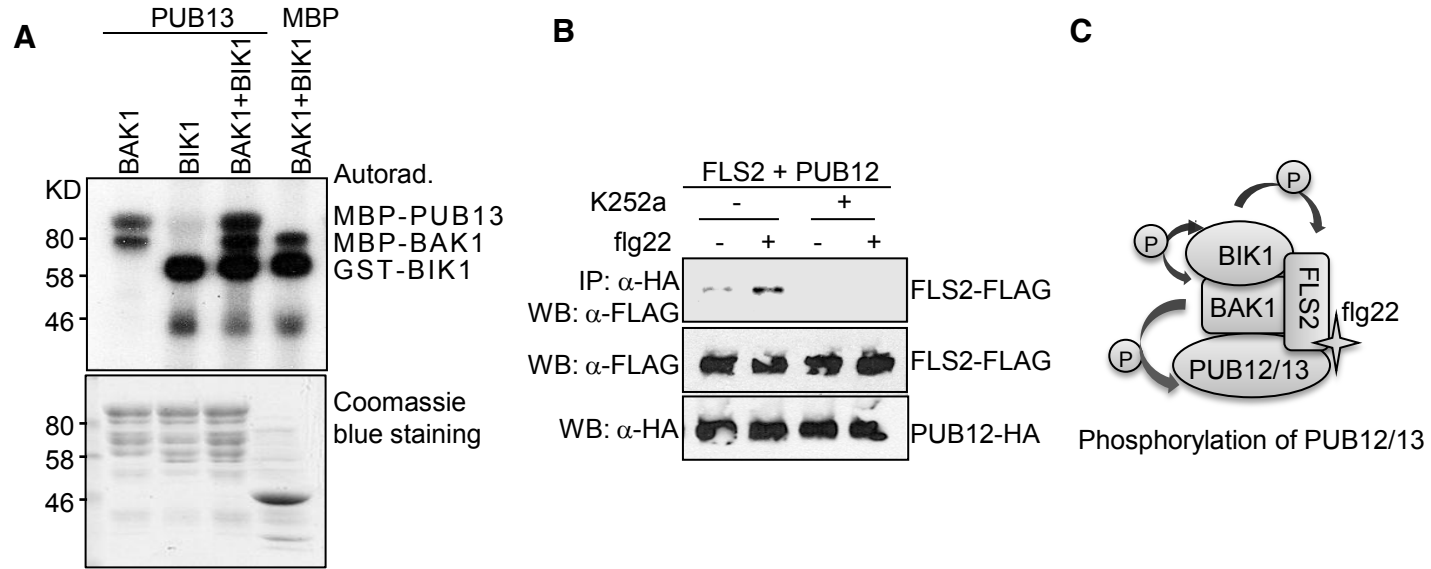


Fig. S3. Phosphorylation events in FLS2/BAK1/BIK1/PUB12/13 complex. (A) BIK1 enhances BAK1 phosphorylation of PUB13. MBP-PUB13, MBP-BAK1 and GST-BIK1 were used in an *in vitro* kinase assay. (B) Kinase inhibitor K252a suppresses FLS2 and PUB12 association. The above experiments were repeated three times with similar results. (C) A model of phosphorylation events in FLS2/BAK1/BIK1/PUB12/13 complex.

Supplemental data

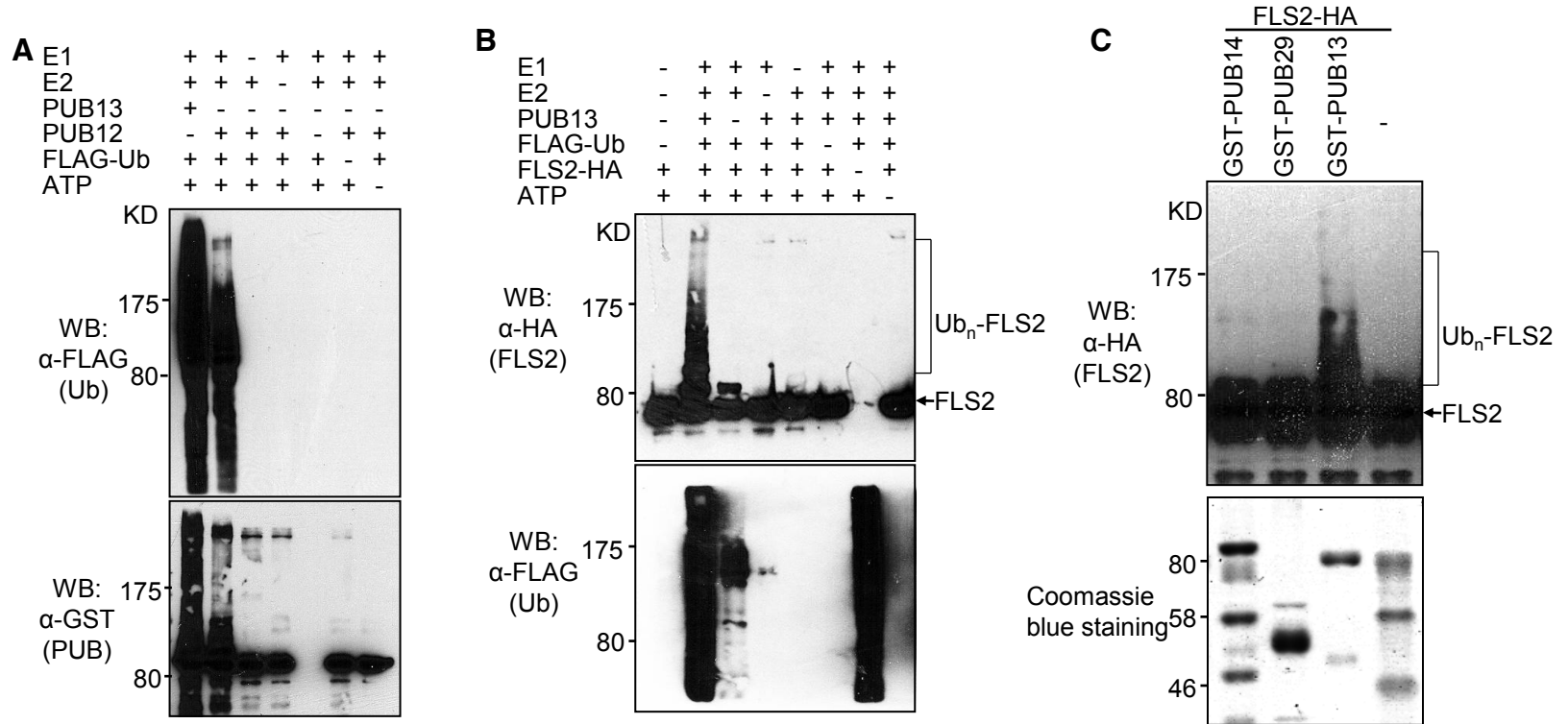


Fig. S4. Auto-ubiquitination of PUB12/13 and the specificity of PUB13 ubiquitination on FLS2. (A) PUB12 and PUB13 possess E3 ubiquitin ligase activity. An *in vitro* ubiquitination assay was performed with GST-PUB12 or GST-PUB13 in combination with E1, E2, FLAG-Ub and ATP. Protein ubiquitination was detected by Western blot with an anti-FLAG or anti-GST antibody. (B) FLS2 ubiquitination by PUB13 in an *in vitro* ubiquitination assay with the components as indicated. (C) An *in vitro* ubiquitination assay was performed with MBP-FLS2-HA, E1, E2, FLAG-Ub, ATP and different GST-PUBs. The bottom panel shows the protein control of different GST-PUBs. The above experiments were repeated three or four times with similar results.

Supplemental data

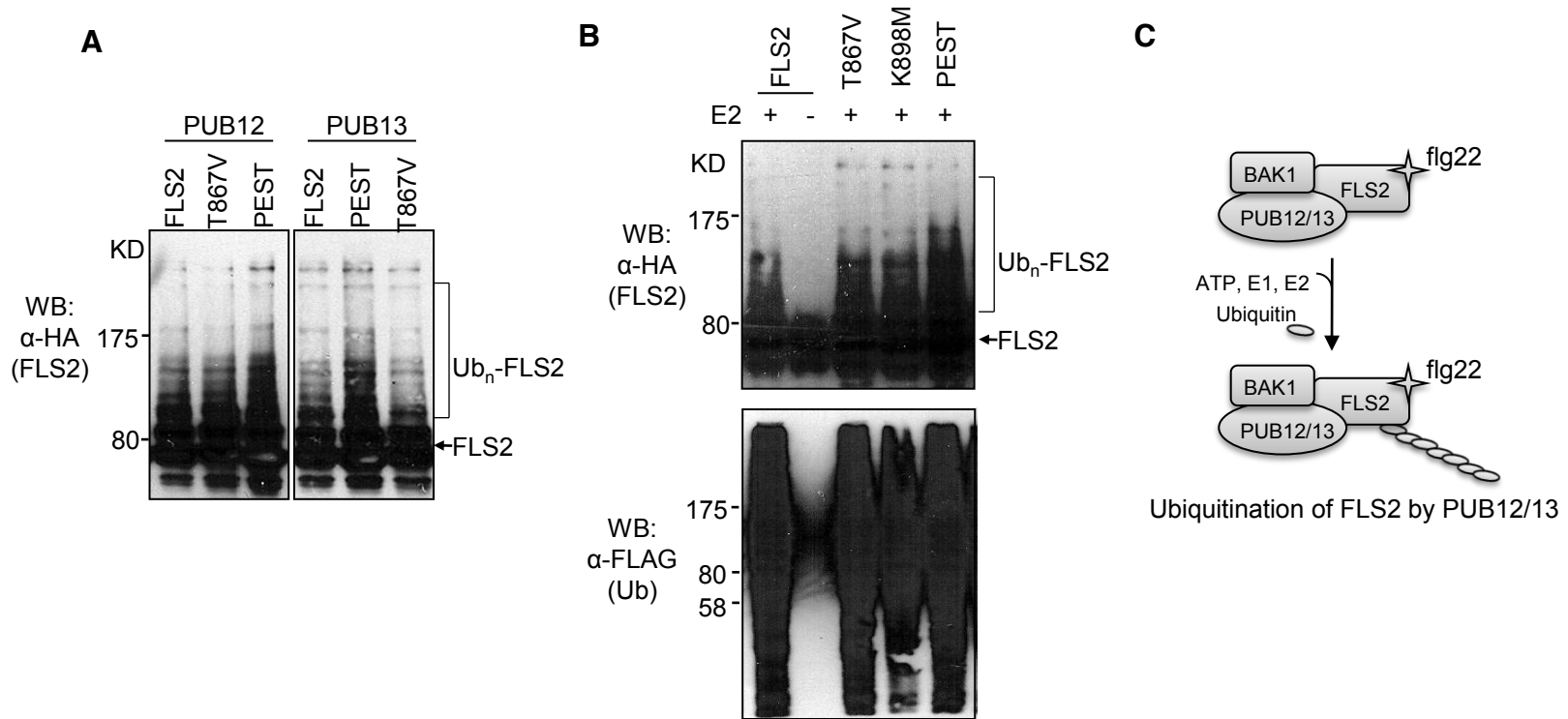


Fig. S5. FLS2 ubiquitination by PUB12/13. (A) PEST and T867 are not required for FLS2 ubiquitination by PUB12 or PUB13. (B) Kinase activity is not required for FLS2 ubiquitination by PUB13. The ubiquitination of MBP-FLS2-HA, MBP-FLS2T867V-HA, MBP-FLS2K898M-HA or MBP-FLS2PEST(P1076A)-HA was tested with GST-PUB12 or GST-PUB13 in an *in vitro* ubiquitination assay. The above experiments were repeated at least three times with similar results. (C) A model of FLS2 ubiquitination by PUB12 and PUB13.

Supplemental data

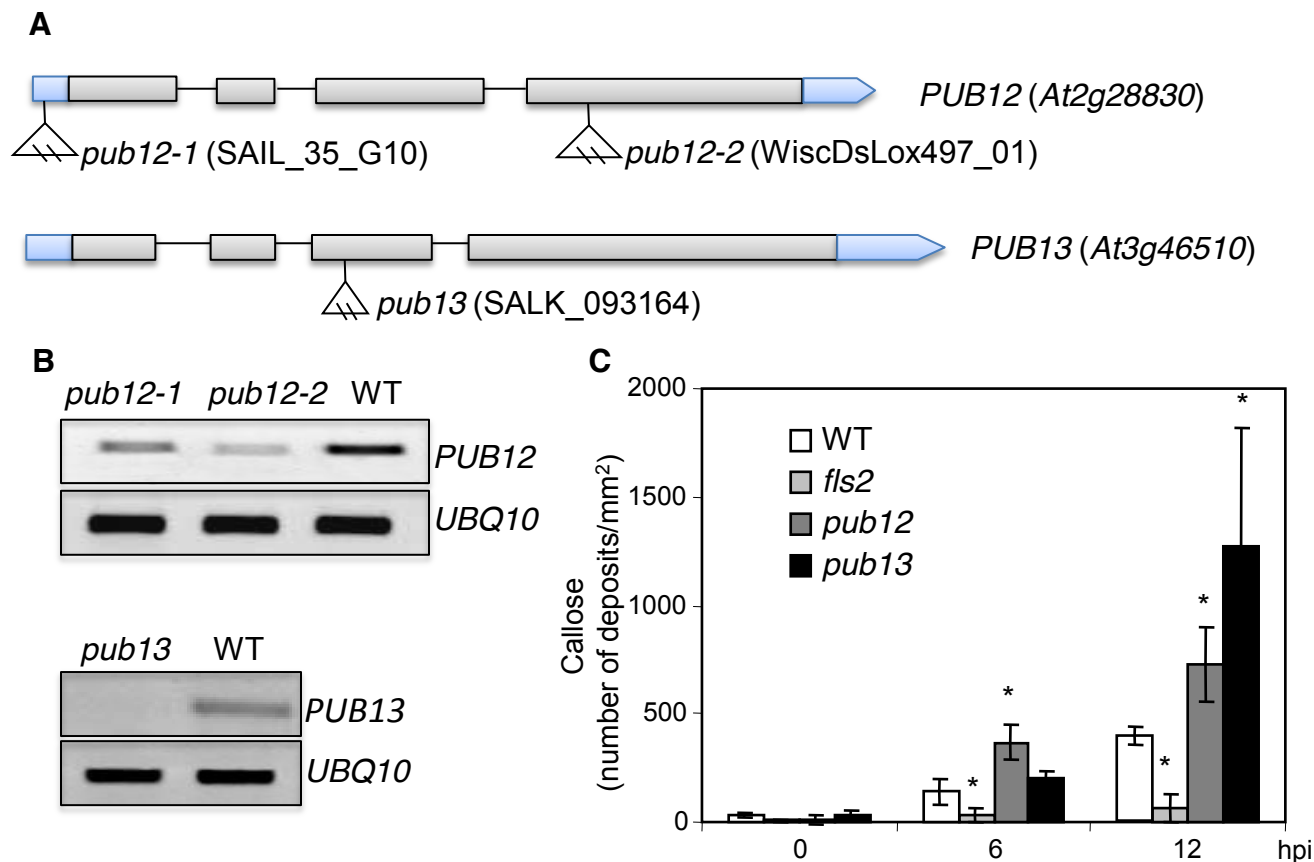


Fig. S6. Analysis of *pub12* and *pub13* mutants. (A) T-DNA insertion sites in *pub* mutants with exons (gray boxes). (B) RT-PCR analysis of *PUB12*, *PUB13* and *UBQ10* (control) in WT and *pub* mutant plants. (C) Statistical analysis of callose deposition in WT, *pub12* and *pub13* mutant plants. The above experiments were repeated three times with similar results.

Supplemental data

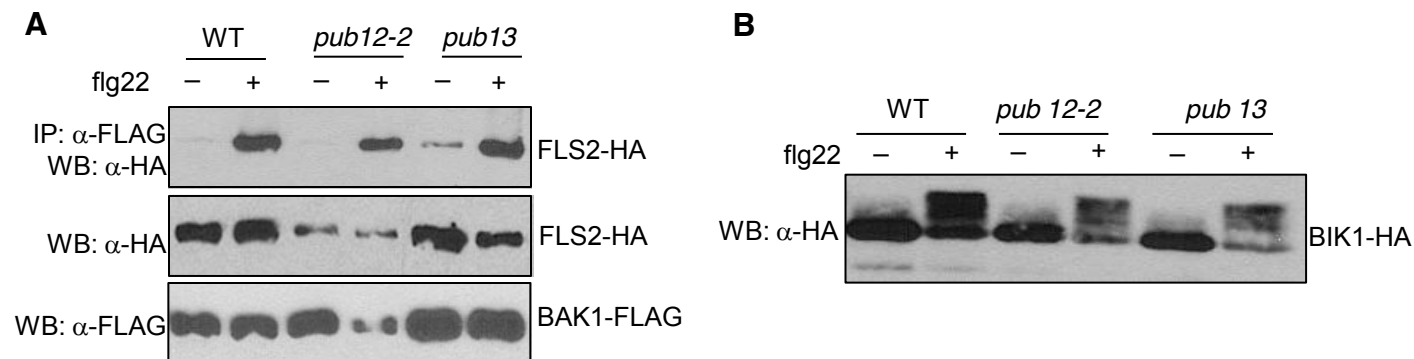


Fig. S7. PUB12 and PUB13 are not required for FLS2/BAK1 association and BIK1 phosphorylation. The protoplasts were isolated from WT, *pub12-2* and *pub13* plants. **(A)** FLS2-HA and BAK1-FLAG were co-expressed in protoplasts for 6 hr before 1 μ M flg22 treatment for 10 min for Co-IP assay. **(B)** BIK1-HA was expressed in protoplasts for 6 hr before 1 μ M flg22 treatment for 10 min for Western blot. The above experiments were repeated three times with similar results.

Supplemental data

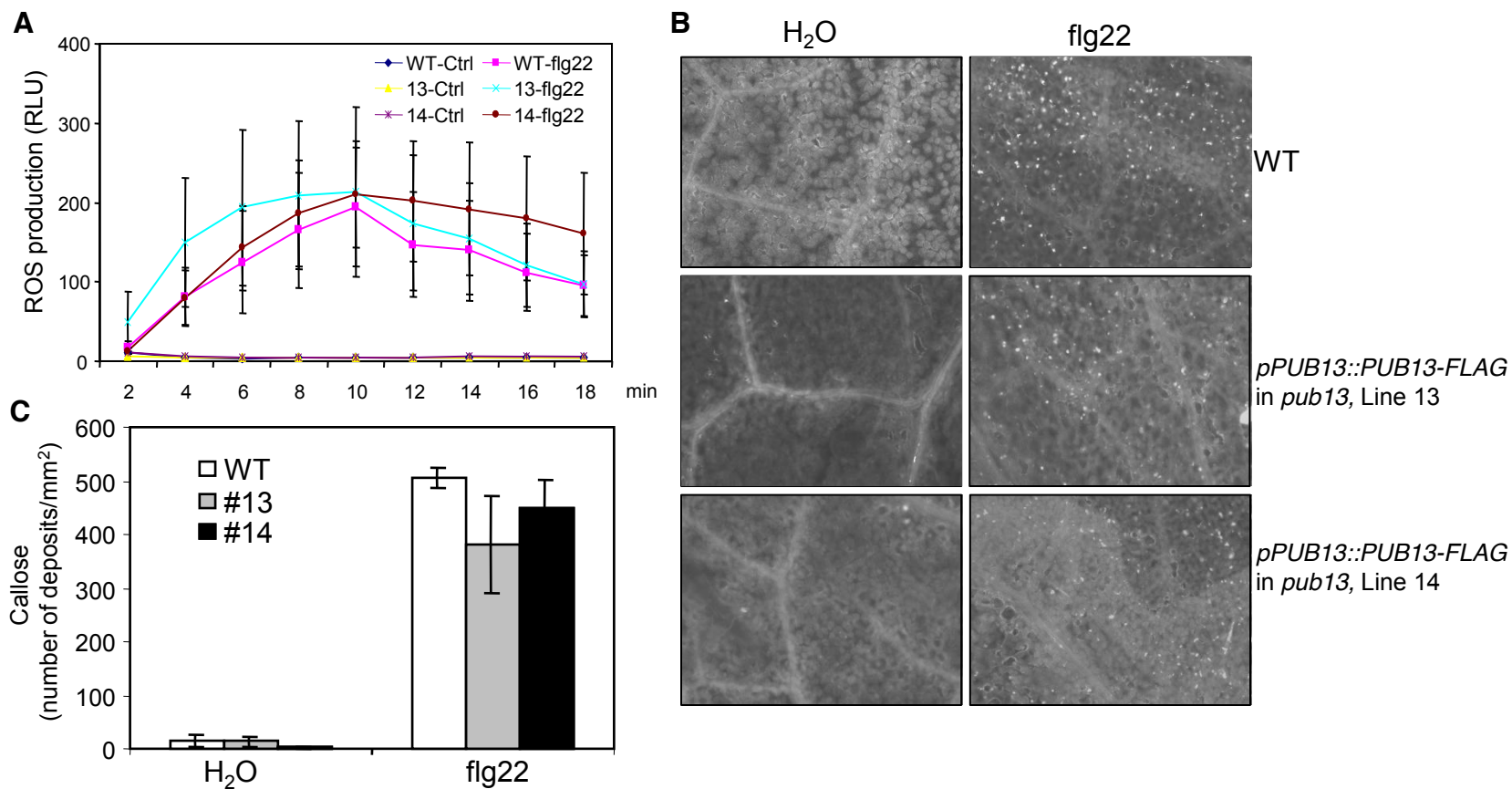


Fig. S8. The *pPUB13::PUB13-FLAG* construct complements *pub13* mutants. (A) flg22-triggered ROS burst in WT and *pPUB13::PUB13-FLAG/pub13* plants. 13 and 14 are two independent transgenic lines. **(B)** flg22-induced callose deposition in WT and *pPUB13::PUB13-FLAG/pub13* plants. Callose deposits were detected 12 hr after 1 μ M flg22 treatment by aniline blue staining. **(C)** Statistical analysis of callose deposition in WT and *pPUB13::PUB13-FLAG/pub13* plants. The above experiments were repeated three times with similar results.

Supplemental data

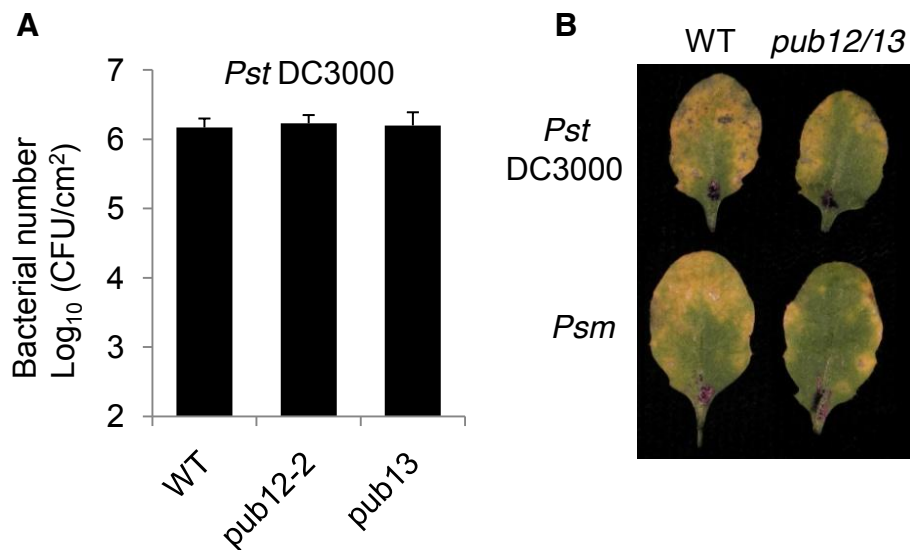


Fig. S9. Bacterial growth assay in *pub12*, *pub13* and *pub12/13* mutants. (A) Four-week-old *Arabidopsis* plants were inoculated with *Pst* DC3000 at a concentration of 5×10^5 cfu/ml. The bacterial counting was performed 3 days post-inoculation (dpi). The data are shown as means \pm standard errors from 3 replicates. (B) Phenotype of bacterial infection in WT and *pub12/13* mutants. Four-week-old *Arabidopsis* plants were inoculated with *Pst* DC3000 and *Psm* at a concentration of 5×10^5 cfu/ml. The picture was taken 6 days post-inoculation. The above experiments were repeated four times with similar results.

Supplemental data

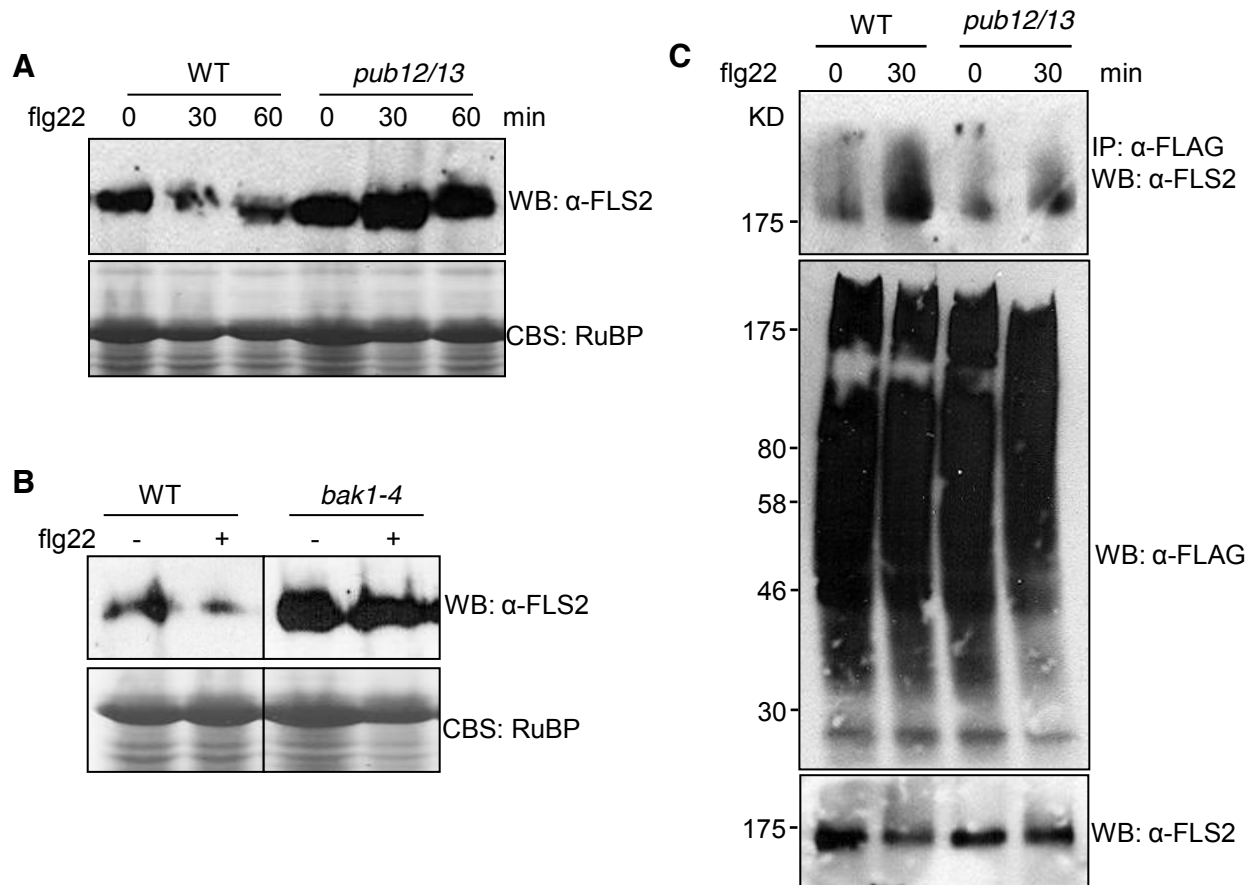


Fig. S10. FLS2 level in *pub12/13* and *bak1* mutants and *in vivo* FLS2 ubiquitination. (A) Four-week-old WT and *pub12/13* *Arabidopsis* plants were inoculated with 1 μ M flg22 for 30 and 60 min. (B) Four-week-old WT and *bak1-4* *Arabidopsis* plants were inoculated with 1 μ M flg22 for 20 min. The protein level of FLS2 was detected by an anti-FLS2 antibody (top panel). The equal protein loading was shown by Coomassie blue staining (CBS) for RuBisCo (bottom panel). (C) *in vivo* FLS2 ubiquitination in WT and *pub12/13* mutant. Protoplasts were transfected with N terminal FLAG-tagged UBQ10, and incubated for 10 hr before 1 μ M flg22 treatment for 30 min. The ubiquitinated FLS2 was detected by an anti-FLS2 antibody after anti-FLAG antibody immunoprecipitation. The total ubiquitinated proteins were detected by an anti-FLAG antibody, and the expression of FLS2 was detected by anti-FLS2. The above experiments were repeated three to four times with similar results.

Supplemental data

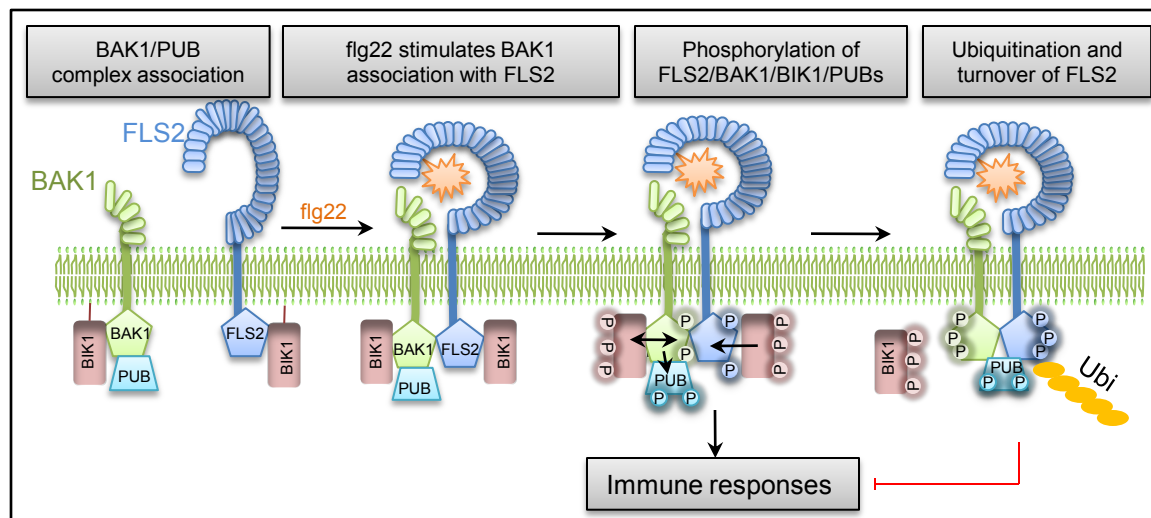


Fig. S11. A proposed model of PUB12/13-mediated ubiquitination of FLS2 in the attenuation of flagellin signaling.

Supplemental data

Table S1. Putative BAK1-interacting proteins from a yeast two-hybrid screen

AGI	Annotation
AT1G01140	CIPK9 (CBL-interacting protein kinase 9)
AT1G20620	Catalase 3
AT1G66200	ATGSR2 (Arabidopsis thaliana glutamine synthase clone R2)
AT1G67880	Glycosyl transferase family 17 protein
AT3G15950	Unknown protein
AT3G46510	PUB13 (Plant U-box 13)
AT3G47910	Ubiquitin thiolesterase
AT4G30996	Unknown protein
AT4G39660	AGT2 (Alanine:glyoxylate aminotransferase 2)
AT5G18230	Transcription regulator NOT2/NOT3/NOT5 family protein

References and Notes

1. O. Takeuchi, S. Akira, Pattern recognition receptors and inflammation. *Cell* **140**, 805 (2010). [doi:10.1016/j.cell.2010.01.022](https://doi.org/10.1016/j.cell.2010.01.022) [Medline](#)
2. T. Boller, G. Felix, A renaissance of elicitors: Perception of microbe-associated molecular patterns and danger signals by pattern-recognition receptors. *Annu. Rev. Plant Biol.* **60**, 379 (2009). [doi:10.1146/annurev.arplant.57.032905.105346](https://doi.org/10.1146/annurev.arplant.57.032905.105346) [Medline](#)
3. J. D. Jones, J. L. Dangl, The plant immune system. *Nature* **444**, 323 (2006). [doi:10.1038/nature05286](https://doi.org/10.1038/nature05286) [Medline](#)
4. P. N. Dodds, J. P. Rathjen, Plant immunity: Towards an integrated view of plant-pathogen interactions. *Nat. Rev. Genet.* **11**, 539 (2010). [doi:10.1038/nrg2812](https://doi.org/10.1038/nrg2812) [Medline](#)
5. L. Gómez-Gómez, T. Boller, FLS2: An LRR receptor-like kinase involved in the perception of the bacterial elicitor flagellin in *Arabidopsis*. *Mol. Cell* **5**, 1003 (2000). [Medline](#)
6. D. Chinchilla *et al.*, A flagellin-induced complex of the receptor FLS2 and BAK1 initiates plant defence. *Nature* **448**, 497 (2007). [doi:10.1038/nature05999](https://doi.org/10.1038/nature05999) [Medline](#)
7. A. Heese *et al.*, The receptor-like kinase SERK3/BAK1 is a central regulator of innate immunity in plants. *Proc. Natl. Acad. Sci. U.S.A.* **104**, 12217 (2007). [doi:10.1073/pnas.0705306104](https://doi.org/10.1073/pnas.0705306104) [Medline](#)
8. J. Li *et al.*, BAK1, an *Arabidopsis* LRR receptor-like protein kinase, interacts with BRI1 and modulates brassinosteroid signaling. *Cell* **110**, 213 (2002). [doi:10.1016/S0092-8674\(02\)00812-7](https://doi.org/10.1016/S0092-8674(02)00812-7) [Medline](#)
9. K. H. Nam, J. Li, BRI1/BAK1, a receptor kinase pair mediating brassinosteroid signaling. *Cell* **110**, 203 (2002). [doi:10.1016/S0092-8674\(02\)00814-0](https://doi.org/10.1016/S0092-8674(02)00814-0) [Medline](#)
10. B. Schulze *et al.*, Rapid heteromerization and phosphorylation of ligand-activated plant transmembrane receptors and their associated kinase BAK1. *J. Biol. Chem.* **285**, 9444 (2010). [doi:10.1074/jbc.M109.096842](https://doi.org/10.1074/jbc.M109.096842) [Medline](#)
11. D. Lu *et al.*, A receptor-like cytoplasmic kinase, BIK1, associates with a flagellin receptor complex to initiate plant innate immunity. *Proc. Natl. Acad. Sci. U.S.A.* **107**, 496 (2010). [doi:10.1073/pnas.0909705107](https://doi.org/10.1073/pnas.0909705107) [Medline](#)
12. J. Zhang *et al.*, Receptor-like cytoplasmic kinases integrate signaling from multiple plant immune receptors and are targeted by a *Pseudomonas syringae* effector. *Cell Host Microbe* **7**, 290 (2010). [doi:10.1016/j.chom.2010.03.007](https://doi.org/10.1016/j.chom.2010.03.007) [Medline](#)
13. S. Robatzek, D. Chinchilla, T. Boller, Ligand-induced endocytosis of the pattern recognition receptor FLS2 in *Arabidopsis*. *Genes Dev.* **20**, 537 (2006). [doi:10.1101/gad.366506](https://doi.org/10.1101/gad.366506) [Medline](#)
14. Materials and methods are available on *Science Online*.
15. D. Yee, D. R. Goring, The diversity of plant U-box E3 ubiquitin ligases: From upstream activators to downstream target substrates. *J. Exp. Bot.* **60**, 1109 (2009). [doi:10.1093/jxb/ern369](https://doi.org/10.1093/jxb/ern369) [Medline](#)

16. C. Azevedo, M. J. Santos-Rosa, K. Shirasu, The U-box protein family in plants. *Trends Plant Sci.* **6**, 354 (2001). [doi:10.1016/S1360-1385\(01\)01960-4](https://doi.org/10.1016/S1360-1385(01)01960-4) [Medline](#)
17. Single-letter abbreviations for the amino acid residues are as follows: A, Ala; C, Cys; D, Asp; E, Glu; F, Phe; G, Gly; H, His; I, Ile; K, Lys; L, Leu; M, Met; N, Asn; P, Pro; Q, Gln; R, Arg; S, Ser; T, Thr; V, Val; W, Trp; and Y, Tyr. In the mutants, other amino acids were substituted at certain locations; for example, H134R indicates that histidine at position 134 was replaced by arginine.
18. V. Göhre *et al.*, Plant pattern-recognition receptor FLS2 is directed for degradation by the bacterial ubiquitin ligase AvrPtoB. *Curr. Biol.* **18**, 1824 (2008). [doi:10.1016/j.cub.2008.10.063](https://doi.org/10.1016/j.cub.2008.10.063) [Medline](#)
19. G. Levkowitz *et al.*, Ubiquitin ligase activity and tyrosine phosphorylation underlie suppression of growth factor signaling by c-Cbl/Sli-1. *Mol. Cell* **4**, 1029 (1999). [doi:10.1016/S1097-2765\(00\)80231-2](https://doi.org/10.1016/S1097-2765(00)80231-2) [Medline](#)
20. A. Craig, R. Ewan, J. Mesmar, V. Gudipati, A. Sadanandom, E3 ubiquitin ligases and plant innate immunity. *J. Exp. Bot.* **60**, 1123 (2009). [doi:10.1093/jxb/erp059](https://doi.org/10.1093/jxb/erp059) [Medline](#)
21. M. Trujillo, K. Shirasu, Ubiquitination in plant immunity. *Curr. Opin. Plant Biol.* **13**, 402 (2010). [doi:10.1016/j.pbi.2010.04.002](https://doi.org/10.1016/j.pbi.2010.04.002) [Medline](#)
22. C. W. Yang *et al.*, The E3 ubiquitin ligase activity of arabidopsis PLANT U-BOX17 and its functional tobacco homolog ACRE276 are required for cell death and defense. *Plant Cell* **18**, 1084 (2006). [doi:10.1105/tpc.105.039198](https://doi.org/10.1105/tpc.105.039198) [Medline](#)
23. R. González-Lamothe *et al.*, The U-box protein CMPG1 is required for efficient activation of defense mechanisms triggered by multiple resistance genes in tobacco and tomato. *Plant Cell* **18**, 1067 (2006). [doi:10.1105/tpc.106.040998](https://doi.org/10.1105/tpc.106.040998) [Medline](#)
24. M. Trujillo, K. Ichimura, C. Casais, K. Shirasu, Negative regulation of PAMP-triggered immunity by an E3 ubiquitin ligase triplet in *Arabidopsis*. *Curr. Biol.* **18**, 1396 (2008). [doi:10.1016/j.cub.2008.07.085](https://doi.org/10.1016/j.cub.2008.07.085) [Medline](#)
25. L. R. Zeng *et al.*, Spotted leaf11, a negative regulator of plant cell death and defense, encodes a U-box/armadillo repeat protein endowed with E3 ubiquitin ligase activity. *Plant Cell* **16**, 2795 (2004). [doi:10.1105/tpc.104.025171](https://doi.org/10.1105/tpc.104.025171) [Medline](#)
26. Y. S. Wang *et al.*, Rice XA21 binding protein 3 is a ubiquitin ligase required for full Xa21-mediated disease resistance. *Plant Cell* **18**, 3635 (2006). [doi:10.1105/tpc.106.046730](https://doi.org/10.1105/tpc.106.046730) [Medline](#)
27. T. H. Chuang, R. J. Ulevitch, Triad3A, an E3 ubiquitin-protein ligase regulating Toll-like receptors. *Nat. Immunol.* **5**, 495 (2004). [doi:10.1038/ni1066](https://doi.org/10.1038/ni1066) [Medline](#)
28. M. A. Lemmon, J. Schlessinger, Cell signaling by receptor tyrosine kinases. *Cell* **141**, 1117 (2010). [doi:10.1016/j.cell.2010.06.011](https://doi.org/10.1016/j.cell.2010.06.011) [Medline](#)
29. L. Shan *et al.*, Bacterial effectors target the common signaling partner BAK1 to disrupt multiple MAMP receptor-signaling complexes and impede plant immunity. *Cell Host Microbe* **4**, 17 (2008). [doi:10.1016/j.chom.2008.05.017](https://doi.org/10.1016/j.chom.2008.05.017) [Medline](#)

30. T. R. Rosebrock *et al.*, A bacterial E3 ubiquitin ligase targets a host protein kinase to disrupt plant immunity. *Nature* **448**, 370 (2007). [doi:10.1038/nature05966](https://doi.org/10.1038/nature05966) [Medline](#)
31. X. Gao *et al.*, *Plant J.* **66**, 293 (2011).
32. L. Wang *et al.*, *Arabidopsis* CaM binding protein CBP60g contributes to MAMP-induced SA accumulation and is involved in disease resistance against *Pseudomonas syringae*. *PLoS Pathog.* **5**, e1000301 (2009). [doi:10.1371/journal.ppat.1000301](https://doi.org/10.1371/journal.ppat.1000301) [Medline](#)
33. P. He *et al.*, Specific bacterial suppressors of MAMP signaling upstream of MAPKKK in *Arabidopsis* innate immunity. *Cell* **125**, 563 (2006). [doi:10.1016/j.cell.2006.02.047](https://doi.org/10.1016/j.cell.2006.02.047) [Medline](#)

Acknowledgments: We thank F. Ausubel, J. Alfano, M. Dickman, and H. Scholthof for critical reading of the manuscript and F. Rolland for the yeast two-hybrid vectors. We also thank the Salk Institute and *Arabidopsis* Biological Resource Center for the *Arabidopsis* T-DNA insertion lines. This work was supported by NSF (IOS-1030250) to L.S. and NIH (R01GM092893) to P.H.

Innate Immunity in Plants Goes to the PUB

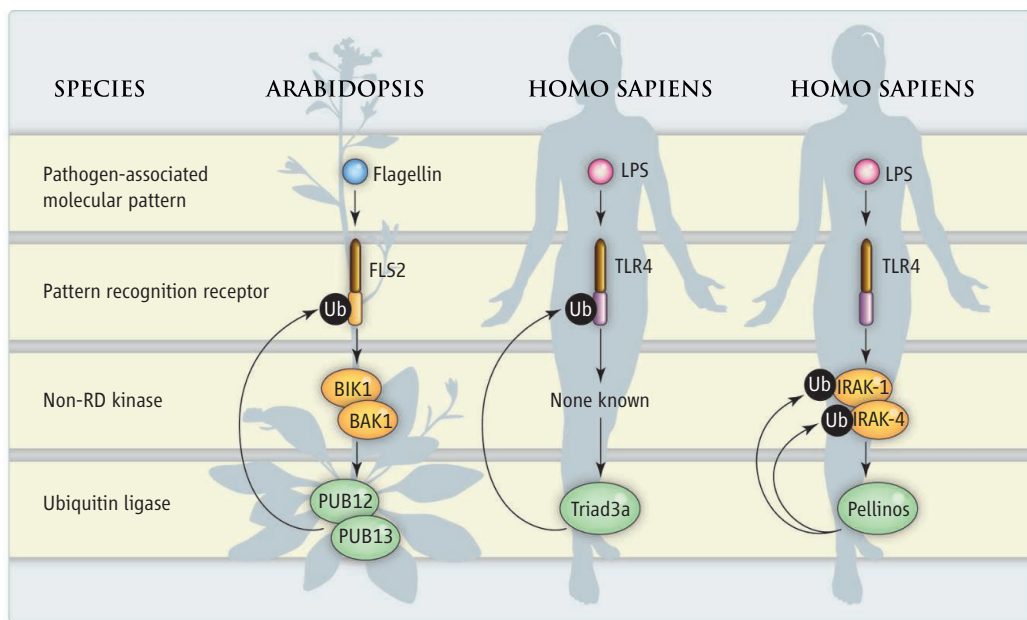
Luke A. J. O'Neill

Every organism has to contend with the risk of infection. To cope, organisms have evolved two types of immune responses: the more recent “adaptive” system, found only in vertebrates; and the more ancient “innate” system, which is present in both plants and animals. Researchers have uncovered remarkable evolutionary conservation of innate immune mechanisms between plants and animals (see the figure). They use similar receptor molecules to sense pathogens, for example, and for immune system signaling. On page 1439 of this issue, Lu *et al.* (1) detail how one plant cell receptor that senses bacterial flagellin triggers an innate immune response. They describe how the activity of the *Arabidopsis* flagellin-sensing receptor 2 (FLS2) is attenuated by a post-translational modification process called ubiquitination and subsequent degradation. The research offers insight into the

general workings of innate immunity and shows that FLS2 activity has clear parallels to the activity of Toll-like receptors (TLRs), an important class of innate immune system receptors. It also indicates that genetic modification to enhance disease resistance in plants is a practical possibility.

FLS2 is a pattern-recognition receptor expressed in the plasma membrane of plant cells. Like TLRs, FLS2 has leucine-rich repeat domains, but also has a kinase domain. This contrasts with TLRs, where the kinases are separate proteins called interleukin-1 receptor-associated kinases (IRAKs). Another receptor-like kinase, BAK1, associates with FLS2 (2), as does a cytoplasmic receptor-like kinase, BIK1, which becomes rapidly phosphorylated when stimulated by the presence of flagellin, the protein that makes up the bacterial flagellum (3). This is

School of Biochemistry and Immunology, Trinity College Dublin, Dublin 2, Ireland. E-mail: laoneill@tcd.ie



Innate immunity, conserved. *Arabidopsis* and humans have evolutionarily conserved innate immune signaling processes that involve a posttranslational modification process called ubiquitination. In *Arabidopsis*, bacterial flagellin is sensed by FLS2, which recruits the non-arginine/aspartate (Non-RD) kinases BAK1 and BIK1. BAK1 phosphorylates and activates PUB12/13, which ubiquitinates (Ub) FLS2 and leads to degradation. In humans, TLR4 senses lipopolysaccharide (LPS). This can activate Triad3a (third column), which ubiquitinates TLR4 and leads to its degradation. TLR4 can also activate IRAK-1 and IRAK-4 (fourth column), which activates nuclear factor kappa B (not shown), and also Pellino proteins (Pellinos), which ubiquitinate the IRAKs and lead to their degradation.

similar to the behavior of the TLRs, which when activated induce rapid phosphorylation of IRAK-1 and IRAK-4 (4).

Lu *et al.* first addressed what other proteins might interact with BAK1 using a technique known as a yeast two-hybrid screen. One interacting protein that they isolated was PUB13, an E3 ubiquitin ligase. It has an Armadillo (ARM) repeat domain, which is also found in sterile-alpha ARM (SARM), a negative regulator of TLR signaling that is highly conserved across species (5). Flagellin strongly enhanced the interaction of PUB13 and FLS2, providing key evidence that the association had a possible role in signaling. PUB12, a close homolog of PUB13, also associated with FLS2. In contrast, a less homologous protein, PUB29, did not, which indicates specificity in the interaction. They then showed that BAK1 was required for the association and identified a preformed complex of BAK1 with PUB12 and PUB13, which was recruited to FLS2 upon flagellin

treatment. Finally, Lu *et al.* addressed what the association of these proteins in signaling might mean functionally. They showed that, after flagellin treatment, BAK1 directly phosphorylated PUB12 and PUB13. BIK1 enhanced this effect, most probably via the direct phosphorylation of BAK1 by BIK1. In addition, they showed that phosphorylation of PUB12 and PUB13 was required for the association between PUB12 and PUB13 and FLS2.

The next step in the pathway was then revealed. Lu *et al.* showed that PUB12 and PUB13 possessed auto-ubiquitination activity and, more importantly, specifically polyubiquitinated FLS2. The parallel with the TLR system is again remarkable. In the case of TLRs, the ubiquitin ligase Triad3a mediates ubiquitination of TLR4 and TLR9 (see the figure), leading to their degradation (6). In the TLR system, however, there is further complexity in the downstream ubiquitination process, with Pellino proteins

acting as ubiquitin ligases for IRAK-4 and IRAK-1, leading to their activation and subsequent degradation (4). This would appear to be a difference with plants, in which the kinases BAK1 and BIK1 do not undergo ubiquitination.

In something of a tour-de-force, the authors then addressed the functional importance of FLS2 ubiquitination by creating plants with mutated PUB12 and PUB13. Flagellin could still induce FLS2-BAK1 association and BIK1 phosphorylation in these plants, which indicated that sensing of flagellin was normal. However, there was a notable boost in host defense responses, including induction of hydrogen peroxide and immune-responsive genes such as *WRKY30*. To create an *Arabidopsis* infection model, Lu *et al.* also generated a double

mutant lacking PUB12 and PUB13. These plants were 10 times as resistant to infection with *Pseudomonas* when compared with wild-type plants. Furthermore, in wild-type plants, flagellin induced the ubiquitination and degradation of FLS2. This did not occur in the mutant plants or in plants with mutant BAK1. The pathway to regulate FLS2 (see the figure) is an important negative feedback process, which, if manipulated (e.g., by mutation or deletion of PUB12/13), will boost host defense in *Arabidopsis*.

The purpose of innate immunity is to sense a displacement from homeostasis and trigger a process to restore the balance. This displacement can be driven by pathogens or tissue injury. In terms of identifying which components are important for this process, 1 billion years of evolutionary conservation

(which is one estimate of when plants and animals diverged) is unlikely to be wrong. We can look forward to further insights from different species, including humans, which will aid efforts to develop therapeutic manipulations of innate immune processes. The goal of such manipulation will be to either boost host defense, or limit the damaging effects of these processes when they go awry.

References

1. D. Lu *et al.*, *Science* **332**, 1439 (2011).
2. D. Chinchilla *et al.*, *Nature* **448**, 497 (2007).
3. D. Lu *et al.*, *Proc. Natl. Acad. Sci. U.S.A.* **104**, 12217 (2010).
4. S. Carpenter, L. A. J. O'Neill, *Biochem. J.* **422**, 1 (2009).
5. M. Carty *et al.*, *Nat. Immunol.* **7**, 1074 (2006).
6. T.-H. Chuang, R. J. Ulevitch, *Nat. Immunol.* **5**, 495 (2004).

10.1126/science.1208448

CELL BIOLOGY

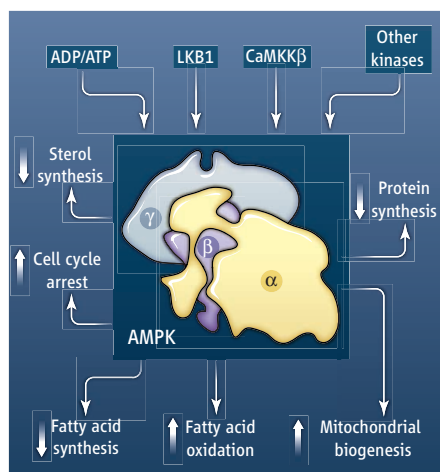
ADaPting to Energetic Stress

Michelle L. Bland and Morris J. Birnbaum

The movement of muscles, the repolarization of neuronal membranes, and the synthesis of cellular building blocks such as proteins and lipids are powered by energy derived from the hydrolysis of adenosine 5'-triphosphate (ATP). Each day, these processes lead to the turnover of 40 kg of ATP in the average adult human being. ATP is indispensable for life, and sophisticated mechanisms for assessing cellular energy status have evolved and been conserved across all eukaryotes. Adenosine 5'-monophosphate (AMP)-activated protein kinase (AMPK; SNF1 in yeast) is a key enzyme that regulates cell energetics. As the name suggests, AMP has long been believed to be the specific metabolite regulating AMPK activity. Oakhill *et al.* on page 1433 in this issue (1) and a recent report by Xiao *et al.* (2) propose an alternative model in which the concentration of intracellular adenosine 5'-diphosphate (ADP) signals the energy status of the cell to AMPK, prompting reevaluation of the pathways that govern adaptation to energetic stress.

AMPK senses the decreased cellular energy charge resulting from increased ATP hydrolysis and initiates appropriate physio-

logical responses to such stress. The AMPK complex consists of a catalytic α subunit, a scaffolding β subunit, and a regulatory γ subunit (see the first figure). The traditional view is that AMP binds to three sites within the γ subunit, slowing dephosphorylation of the critical α -subunit activation loop residue threonine-172 (Thr¹⁷²). Phosphorylated AMPK can be further activated directly by AMP binding, and AMP-bound AMPK pro-



AMPK signaling. AMPK is activated by phosphorylation by LKB1 and CaMKKβ and perhaps other kinases. AMPK integrates information about cellular energy status with input from multiple signaling pathways to direct cell metabolism and growth.

What is the true activator of a key enzyme that controls cell energetics?

vides a better substrate for the upstream kinases liver kinase B1 (LKB1) and calcium- and calmodulin-dependent protein kinase kinase β (CaMKKβ), though the latter mechanism is controversial. Unlike AMP, ADP is not an allosteric regulator of AMPK activity; consequently, its potential function in the control of AMPK phosphorylation has been largely overlooked. However, Oakhill *et al.* and Xiao *et al.* demonstrate that like AMP, ADP protects AMPK from dephosphorylation at Thr¹⁷² (see the second figure). Because intracellular ADP concentrations generally exceed those of AMP, it would appear that ADP is the physiological determinant of the state of AMPK phosphorylation. Perhaps ADP protects AMPK phosphorylation, allowing allosteric activation once AMP production increases during extreme metabolic stress.

During much of its history, AMPK has been regarded as a sensor of energetic stress—that is, an emergency valve for cells in trouble. Most experiments addressing the physiological role of AMPK were based on its activation by cellular toxins that block ATP synthesis or compounds such as aminoimidazole carboxamide ribonucleotide (AICAR) that mimic AMP. Such studies showed that AMPK activates processes that promote ATP generation such as glucose transport (in muscle) and fatty

Institute for Diabetes, Obesity and Metabolism, University of Pennsylvania School of Medicine, Philadelphia, PA 19104, USA. E-mail: birnbaum@mail.med.upenn.edu